Sialidase down-regulation reduces non-HDL cholesterol, inhibits leukocyte transmigration, and attenuates atherosclerosis in ApoE knockout mice

Received for publication, June 26, 2018, and in revised form, August 1, 2018 Published, Papers in Press, August 10, 2018, DOI 10.1074/jbc.RA118.004589

Elizabeth J. White[‡1], Gabriel Gyulay[‡], Šárka Lhoták[§], Magdalena M. Szewczyk[‡], Taryne Chong[‡], Mark T. Fuller[¶‖2], Omid Dadoo[¶‖], Alison E. Fox-Robichaud[§‖], Richard C. Austin[§‖], Bernardo L. Trigatti[¶‖], and Suleiman A. Igdoura[‡3]**

*From the Departments of [‡]Biology, [¶]Biochemistry and Biomedical Sciences, **Pathology and Molecular Medicine, and [‖]Thrombosis and Atherosclerosis Research Institute, McMaster University, Hamilton, Ontario L8S 4K1 and the [§]Department of Medicine, Division of Nephrology, McMaster University, St. Joseph's Healthcare and Hamilton Centre for Kidney Research, Hamilton, Ontario L8N 4A6 , Canada*

Edited by Gerald W. Hart

Atherosclerosis is a complex disease that involves alterations in lipoprotein metabolism and inflammation. Protein and lipid glycosylation events, such as sialylation, contribute to the development of atherosclerosis and are regulated by specific glycosidases, including sialidases. To evaluate the effect of the sialidase neuraminidase 1 (NEU1) on atherogenesis, here we generated apolipoprotein E (ApoE)-deficient mice that express hypomorphic levels of NEU1 (*Neu1^{hypo}Apoe$^{-/-}$*). We found that the hypomorphic NEU1 expression in male *Apoe$^{-/-}$* mice reduces serum levels of very-low-density lipoprotein (VLDL) and LDL cholesterol, diminishes infiltration of inflammatory cells into lesions, and decreases aortic sinus atherosclerosis. Transplantation of *Apoe$^{-/-}$* bone marrow (BM) into *Neu1^{hypo}Apoe$^{-/-}$* mice significantly increased atherosclerotic lesion development and had no effect on serum lipoprotein levels. Moreover, *Neu1^{hypo}Apoe$^{-/-}$* mice exhibited a reduction in circulating monocyte and neutrophil levels and had reduced hyaluronic acid and P-selectin adhesion capability on monocytes/neutrophils and T cells. Consistent with these findings, administration of a sialidase inhibitor, 2-deoxy-2,3-dehydro-*N*-acetylneuraminic acid, had a significant anti-atherogenic effect in the *Apoe$^{-/-}$* mice. In summary, the reduction in NEU1 expression or function decreases atherosclerosis in mice via its significant effects on lipid metabolism and inflammatory processes. We conclude that NEU1 may represent a promising target for managing atherosclerosis.

Atherosclerosis generates the progressive luminal narrowing of arteries, which is the underlying cause of myocardial infarction and stroke. Formation of atherosclerotic plaques involve the accumulation of cholesterol and inflammatory cells in the subendothelial space of the vessel intima (1). The inhibition of inflammatory cell proliferation, activation, trans-endothelial migration, and pro-inflammatory cytokine secretion as well as the reduction of serum lipoprotein levels are all key factors in decreasing the formation of atherosclerotic lesions. Despite these well-established events that contribute to atherogenesis, the mechanisms that underlie these processes have not been fully elucidated. This study examines how the control of protein and lipid glycosylation contributes to the development of atherosclerosis.

Sialic acids are terminal sugars that provide switches to control the function of cell-surface and soluble glycoproteins. These sugars are frequently in α2,3- or α2,6-linkages with galactose, on *N*- and *O*-linked oligosaccharides of both glycoproteins and glycolipids. The levels of sialic acid are tightly regulated by the activities of sialyltransferases and sialidases. Given the important role of sialidase during immune cell development and activation and the inducible activities of sialidases (2–6), we sought to investigate if sialidase plays a role in the development of cardiovascular disease (7). The four known mammalian sialidases differ in their subcellular localization, including lysosomal/plasma membrane NEU1 (8, 9), cytosolic NEU2 (10), plasma membrane NEU3 (11), and mitochondrial NEU4 (12). We previously demonstrated that human NEU1 overexpression reduces cell-surface sialylation *in vitro* (13), which provides evidence that NEU1 controls the sialylation status of cell-surface molecules. Sialidase has also been implicated in the regulation of cell-adhesion molecules, including CD43 (14), and PSGL-1 and CD44 (14, 15), which are involved in leukocyte extravasation during vessel inflammation.

The presence of sialic acid on apolipoproteins has been implicated in their binding, secretion, and plasma clearance (16). Desialylation of ApoB increases the clearance of LDL[4] (17, 18). The LDL receptor (LDLR) is also sialylated (19) and we

This work was supported by Heart & Stroke Foundation of Canada (HSF) grants (to S. A. I.). The authors declare that they have no conflicts of interest with the contents of this article.

[1] Recipient of a Canadian Institutes of Health Research (CIHR) postdoctoral fellowship.

[2] Recipient of a CIHR studentship.

[3] To whom correspondence should be addressed: McMaster University, 1280 Main St. W. LSB 335, Hamilton, Ontario L8S 4K1, Canada. Tel.: 905-525-9140 (ext. 27729); Fax: 905-522-6066; E-mail: igdoura@mcmaster.ca.

[4] The abbreviations used are: LDL, low density lipoprotein; Ad, adenovirus; *Apoe*, apolipoprotein E; β-Gal, β-galactosidase; BM, bone marrow; BMDM, bone marrow derived macrophages; DANA, 2-deoxy-2,3-dehydro-*N*-acetylneuraminic acid; HA, hyaluronic acid; IDL, intermediate density lipoprotein; IFNγ, interferon γ; LDLR, low density lipoprotein receptor; MALII, *M. amurensis* II lectin; MCP-1, monocyte chemoattractant protein 1; NEU1, neuraminidase 1; NK, natural killer; PNA, peanut agglutinin; SMA, smooth muscle actin; SNA, *S. nigra* lectin; TG, triglyceride; TNFα, tumor necrosis factor α; VCAM-1, vascular cell adhesion molecule 1; VLDL, very low density lipoprotein; IL, interleukin; GAPDH, glyceraldehyde-3-phosphate dehydrogenase; HRP, horseradish peroxidase; LPS, lipopolysaccharide.

have shown that NEU1 expression can affect lipoprotein metabolism *in vivo* (20). Thus, mouse and human sialidases both play an important role in lipoprotein metabolism.

Sialidase deficiency in SM/J mice leads to higher sialic acid content of liver and blood cell glycoproteins (21). Carrillo *et al.* (22) identified a Leu-209 to Ile mutation within the ORF of the *Neu1* gene that significantly reduces NEU1 activity in SM/J mice. We generated hypomorphic NEU1 mice ($Neu1^{hypo}$) by backcrossing SM/J mice to C57BL/6 mice and identified an additional mutation in the promoter of the *Neu1* gene that contributes to the hypomorphic phenotype (23). The $Neu1^{hypo}$ mouse is a valuable model because it does not produce the deadly lysosomal storage disease phenotype observed in $Neu1^{-/-}$ mice (24). In our previous work, we showed that $Neu1^{hypo}$ mice have elevated levels of hepatic cholesterol and triglycerides (TGs) but lower microsomal triglyceride transfer protein (MTP) expression and lower VLDL-TG production rate, which can be reversed by rescuing the NEU1 expression (20). Furthermore, hypomorphic sialidase expression stabilizes hepatic LDLR protein expression, which enhances LDL uptake. It is still unclear, however, whether NEU1-dependent modulation of lipoprotein production and clearance affects the course of atherosclerosis.

Results

NEU1 expression and activity are reduced in $Neu1^{hypo}Apoe^{-/-}$ mice

To determine whether sialidase plays a role locally within the atherosclerotic lesions and within the liver, we examined both NEU1 protein expression and sialidase activity in these tissues. There was no difference in the expression of the lower molecular weight form of NEU1 protein in the thoracic aorta of $Apoe^{-/-}$ and $Neu1^{hypo}Apoe^{-/-}$ mice (Fig. 1, *A* and *B*). In liver tissue, the NEU1 protein existed as two forms, including the ~46 kDa low molecular weight form observed in the aorta, as well as a slightly larger molecular weight form at ~48 kDa (Fig. 1*A*). This larger molecular weight form of NEU1 in liver tissue was expressed at a significantly lower level in the $Neu1^{hypo}Apoe^{-/-}$ mice compared with $Apoe^{-/-}$ mice (Fig. 1*C*). Although we measured no difference in total NEU1 expression in the thoracic aorta, we observed lower NEU1 immunoreactivity in lesions of the aortic sinus and also within the liver of $Neu1^{hypo}Apoe^{-/-}$ mice compared with $Apoe^{-/-}$ mice (Fig. 1, *D–G*). Given that NEU1 activity varies from tissue to tissue in the hypomorphic Neu1 mouse (20), we measured sialidase activity in aorta, liver, and bone marrow- derived macrophages (BMDMs). Sialidase activity was significantly reduced in the aorta, liver, and macrophages of $Neu1^{hypo}Apoe^{-/-}$ mice compared with $Apoe^{-/-}$ mice (Fig. 1, *H–J*). Together, the differences between the NEU1 expression and activity data in the aorta of $Neu1^{hypo}Apoe^{-/-}$ mice suggest that the $Neu1^{hypo}$ mutation in the enzyme active site has the dominant effect in the aorta tissue, whereas both $Neu1^{hypo}$ mutations in the promoter and enzyme active site of the gene contribute to NEU1 deficiency in the liver. These data confirm that NEU1 deficiency would have local effects in cells and tissues involved in lesion formation and lipid metabolism.

Hypomorphic NEU1 expression reduces serum and hepatic cholesterol levels

To assess the impact of reduced sialidase expression on serum lipid profile, serum from unfasted mice was fractionated using fast protein liquid chromatography (FPLC). Serum cholesterol associated with VLDL- and IDL/LDL-sized particles was significantly lower in $Neu1^{hypo}Apoe^{-/-}$ mice compared with $Apoe^{-/-}$ mice (Fig. 2*A*). The observed reduction in VLDL and IDL/LDL fractions in $Neu1^{hypo}Apoe^{-/-}$ males compared with $Apoe^{-/-}$ male mice led us to measure the total hepatic and serum lipid levels in these mice. Total hepatic cholesterol and free cholesterol were decreased in $Neu1^{hypo}Apoe^{-/-}$ mice compared with $Apoe^{-/-}$ mice, whereas hepatic cholesteryl esters and hepatic TGs remained unchanged (Table 1). Serum cholesterol concentrations (including total, free, and esters) were strikingly decreased in $Neu1^{hypo}Apoe^{-/-}$ mice compared with $Apoe^{-/-}$ mice but serum TG was not changed (Table 1). We saw similar reductions in serum cholesterol but not TG levels in $Neu1^{hypo}Apoe^{-/-}$ mice compared with $Apoe^{-/-}$ mice that had been fed a high-fat atherogenic diet for 4 weeks (data not shown).

Hypomorphic NEU1 expression reduces hepatic VLDL-lipid production rate

To examine the effect of VLDL-TG production on VLDL levels in $Neu1^{hypo}Apoe^{-/-}$ mice, the hepatic VLDL-TG production was measured *in vivo* over 4 h (Fig. 2*B*). Our results indicate a lower production rate of VLDL-TG in $Neu1^{hypo}Apoe^{-/-}$ mice compared with $Apoe^{-/-}$ mice (Fig. 2*C*). In fact, $Neu1^{hypo}Apoe^{-/-}$ mice show significantly reduced levels of VLDL-TG production at hours 3 and 4 compared with $Apoe^{-/-}$ mice.

Hypomorphic NEU1 expression reduces atherosclerosis in $Apoe^{-/-}$ mice

We utilized 7-month-old $Neu1^{hypo}Apoe^{-/-}$ and $Apoe^{-/-}$ mice to investigate the effect of reduced sialidase expression on the size of atherosclerotic lesions at the aortic sinus. Our results demonstrate that $Neu1^{hypo}Apoe^{-/-}$ mice show a significantly reduced atherosclerotic lesion size (>50% reduction) compared with the $Apoe^{-/-}$ mice (Fig. 2, *D* and *E*). The volume of atherosclerotic lesions was also measured and found to be significantly lower in $Neu1^{hypo}Apoe^{-/-}$ mice compared with $Apoe^{-/-}$ mice (Fig. 2*F*). We saw a similar degree of reduction in aortic sinus atherosclerosis levels in $Neu1^{hypo}Apoe^{-/-}$ mice compared with $Apoe^{-/-}$ mice that had been fed a high-fat atherogenic diet for 4 weeks (data not shown). Sudan IV staining of the *en face* preparation of the thoraco-abdominal aorta from chow-fed mice was also measured to clarify the effect of hypomorphic sialidase expression on the extent of lipid content of aortic lesions (Fig. 2*G*). The lipid content of aortic lesions in $Neu1^{hypo}Apoe^{-/-}$ mice was approximately one-half of the area in $Apoe^{-/-}$ mice (Fig. 2*H*).

Hypomorphic NEU1 expression reduces the number of macrophages, T cells, and smooth muscle cells within the aortic root

Actively progressing atherosclerotic lesions consist mostly of macrophages, T cells, and smooth muscle cells. We immuno-

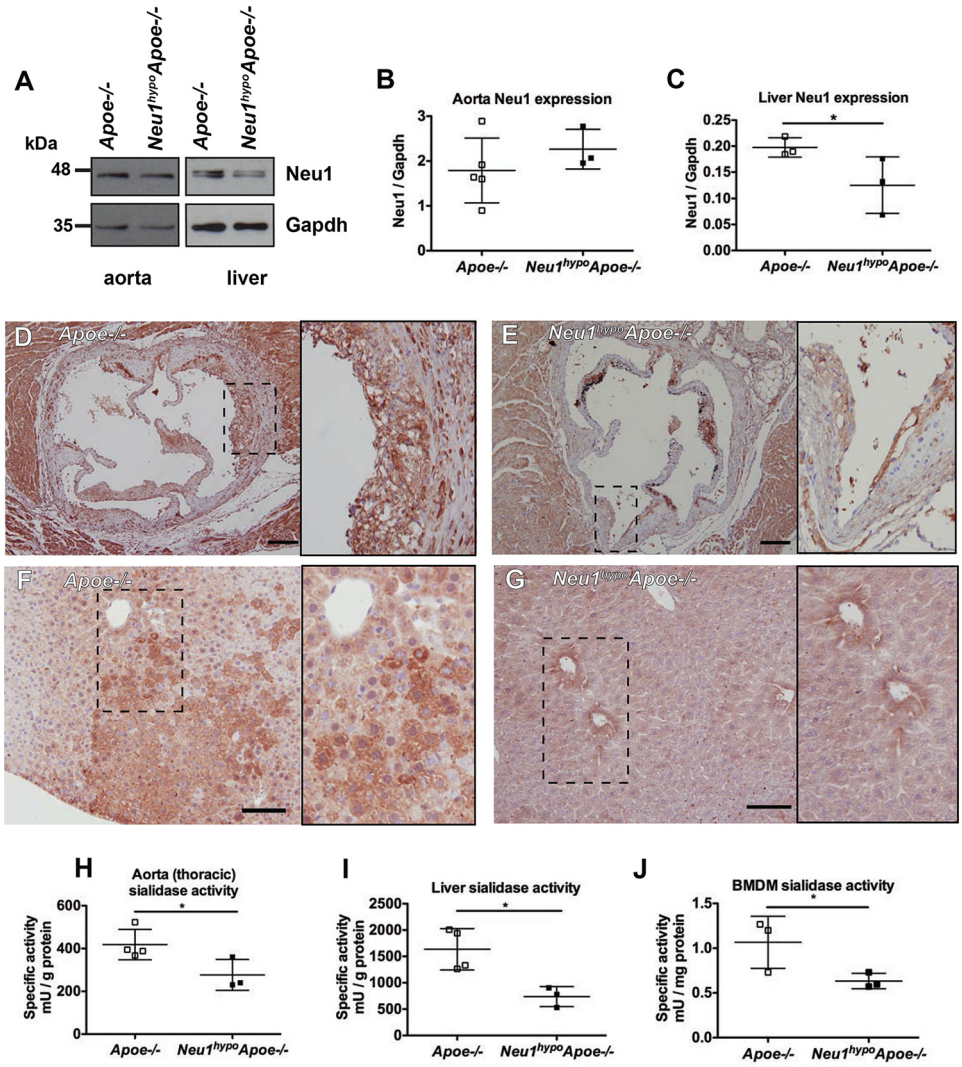

Figure 1. NEU1 protein expression and activity levels in *Apoe*$^{-/-}$ and *Neu1*^{hypo}*Apoe*$^{-/-}$ tissues. *A,* representative Western blotting results are presented, with densitometry (*B* and *C*) carried out for $n = 3$–5 of each group. *B,* expression of NEU1 protein was not significantly different in aortic tissue, which only expressed the lower M_r sized band of NEU1 compared with the two forms observed in liver tissue. *C,* NEU1 protein expression (higher M_r form) was significantly less in the liver of *Neu1*^{hypo}*Apoe*$^{-/-}$ mice compared with *Apoe*$^{-/-}$ mice. *, $p < 0.05$. *D–G,* NEU1 localization was examined by immunohistochemistry in the aortic sinus (*D* and *E*) and liver (*F* and *G*) of *Apoe*$^{-/-}$ and *Neu1*^{hypo}*Apoe*$^{-/-}$ mice. Images show an overview and an *inset* showing detail of the region delineated with a *dotted line*. NEU1 immunoreactivity was reduced in both aortic root and liver of *Neu1*^{hypo}*Apoe*$^{-/-}$ mice compared with *Apoe*$^{-/-}$ mice. *D* and *E, scale bar* = 200 μm; *F* and *G, scale bar* = 100 μm. *H–J,* sialidase activity was measured in the aorta (*H*), liver (*I*), and in cultured bone marrow-derived macrophages (*J*) of *Apoe*$^{-/-}$ and *Neu1*^{hypo}*Apoe*$^{-/-}$ mice. Aorta and liver tissues were freshly isolated from *Apoe*$^{-/-}$ mice ($n = 4$) and *Neu1*^{hypo}*Apoe*$^{-/-}$ mice ($n = 3$) between the ages of 233 and 246 days. Bone marrow was cultured from 60-day-old mice, in the presence of M-CSF for 9 days. 1 milliunit = 1 nmol of liberated 4-umbelliferone/h.

stained aortic root sections for Mac3$^+$, CD3$^+$, and SMA$^+$ cells to measure the abundance of macrophages, T cells, and smooth muscle cells, respectively, within atherosclerotic plaques. The number of Mac3$^+$ macrophages per lesion area in *Neu1*^{hypo}*Apoe*$^{-/-}$ mice was reduced by 41% compared with *Apoe*$^{-/-}$ mice (Fig. 3, *A–C*). There was also a significant reduction in the number of CD3$^+$ T cells per lesion area of *Neu1*^{hypo}*Apoe*$^{-/-}$ males compared with *Apoe*$^{-/-}$ controls (Fig. 3, *D–F*). The area of SMA$^+$ smooth muscle cells within the media layer of the aortic root of *Neu1*^{hypo}*Apoe*$^{-/-}$ mice was also significantly lower than *Apoe*$^{-/-}$ mice (Fig. 3, *G–I*). This implicates NEU1 sialidase in the development of the medial layer of the vessel wall. MCP-1 and VCAM expression in the plaque were not significantly different in *Neu1*^{hypo}*Apoe*$^{-/-}$ mice compared with *Apoe*$^{-/-}$ mice (Fig. 3, *J–L* and *M–O,* respectively). Therefore, the *Neu1*^{hypo}*Apoe*$^{-/-}$ mice display fewer macrophages, T cells, and smooth muscle cells in the aortic root compared with the *Apoe*$^{-/-}$ mice, implying a reduced degree of inflammation and cell recruitment within the plaque.

Transplantation of hypomorphic NEU1 BM protects mice from atherosclerosis with no effect on serum lipid levels

To clarify whether sialidase expression in the hematopoietic lineages contributes significantly to atherogenesis and whether the reduced serum lipid levels affect lesion development, we transplanted *Neu1*^{hypo}*Apoe*$^{-/-}$ mice with *Apoe*$^{-/-}$ BM or *Neu1*^{hypo}*Apoe*$^{-/-}$ BM as a control. Transplantation of male *Apoe*$^{-/-}$ BM into male *Neu1*^{hypo}*Apoe*$^{-/-}$ mice led to an increased atherosclerotic-lesion area and volume compared with the transplantation of male *Neu1*^{hypo}*Apoe*$^{-/-}$ BM into male *Neu1*^{hypo}*Apoe*$^{-/-}$ mice (Fig. 4, *A–D*). Thus, rescu-

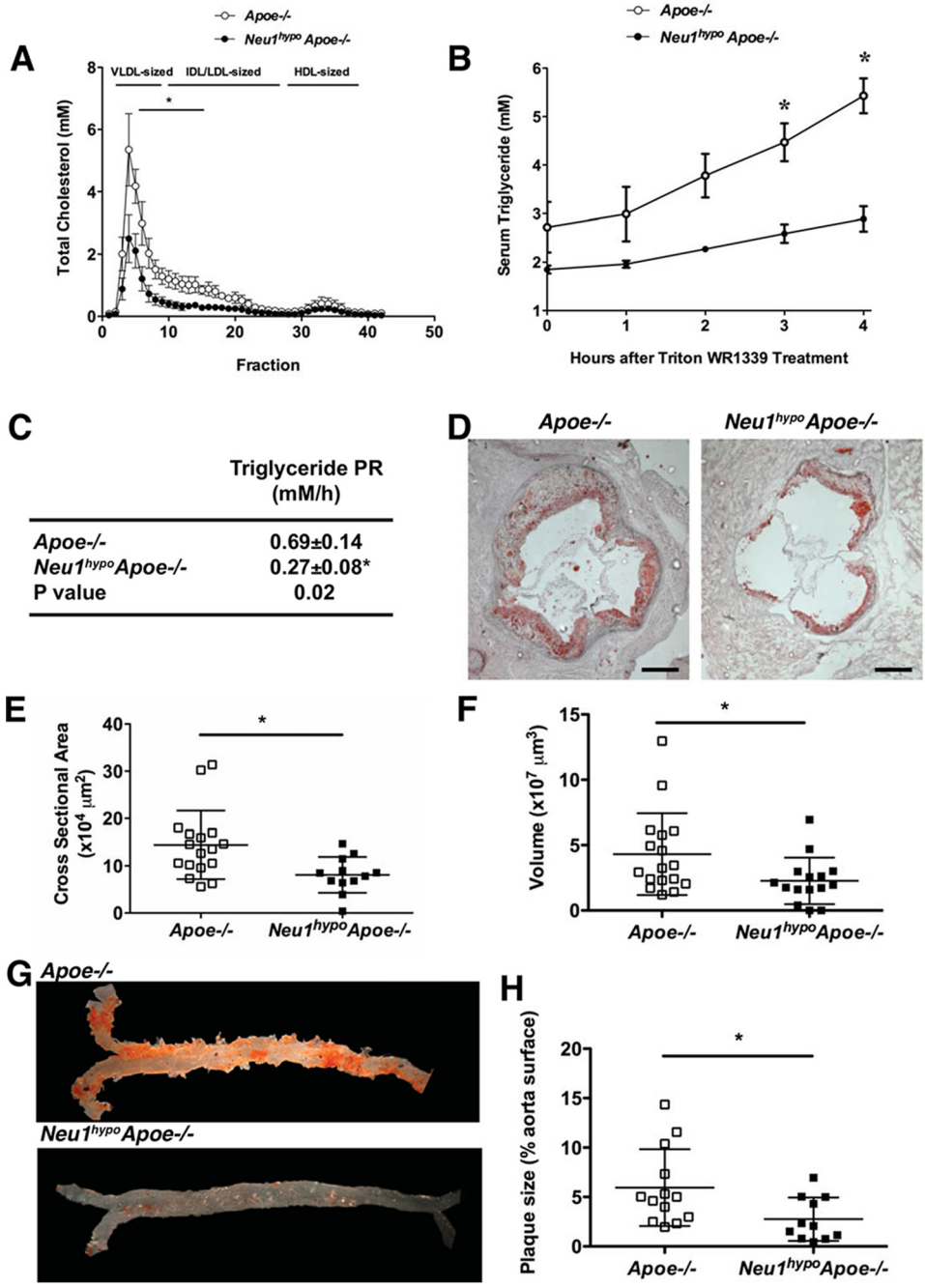

Figure 2. FPLC cholesterol profiles, *in vivo* hepatic VLDL-TG secretion, and atherosclerotic lesion analysis for regular chow-fed *Apoe*$^{-/-}$ and *Neu1*^{hypo}*Apoe*$^{-/-}$ mice. *A,* the serum cholesterol FPLC profiling revealed a significant decrease in VLDL- and LDL-sized particles in 7-month-old, unfasted male *Neu1*^{hypo}*Apoe*$^{-/-}$ mice ($n = 3$) compared with *Apoe*$^{-/-}$ controls ($n = 3$). *B,* after fasting overnight, male *Apoe*$^{-/-}$ ($n = 4$) and male *Neu1*^{hypo}*Apoe*$^{-/-}$ mice ($n = 4$) were injected with Triton WR1339 (500 mg/kg). Serum samples were collected before injection (time 0) and at 1, 2, 3, and 4 h after Triton WR1339 administration. There was a significant decrease in the VLDL-TG concentration in the hypomorphic sialidase mice compared with controls. *C,* the *in vivo* hepatic VLDL-TG production rate, calculated by linear regression from the slope of the VLDL-TG level *versus* the time curve in *B*. There was a significant decrease in the hepatic VLDL-TG production rate (*PR*) in *Neu1*^{hypo}*Apoe*$^{-/-}$ mice compared with *Apoe*$^{-/-}$ mice. This difference indicates that hypomorphic sialidase expression decreased hepatic VLDL secretion. The values are displayed as mean ± S.E. *D,* representative cross-sections of the aortic sinus from male *Apoe*$^{-/-}$ and *Neu1*^{hypo}*Apoe*$^{-/-}$ mice fed a regular chow diet at 7 months of age. Sections were stained with Oil Red O for neutral lipids and counterstained with hematoxylin for nuclei. *Scale bar* = 200 μm. The atherosclerotic lesions were significantly reduced in male *Neu1*^{hypo}*Apoe*$^{-/-}$ mice ($n = 15$) compared with male *Apoe*$^{-/-}$ mice ($n = 17$) both in area (*E*) and volume (*F*). Individual data are displayed with mean ± S.D. *G* and *H,* representative Sudan IV staining of aortas from male *Apoe*$^{-/-}$ and *Neu1*^{hypo}*Apoe*$^{-/-}$ mice (*G*) and quantification of plaque size as a percentage of aorta surface (*H*). Plaque size was significantly reduced in the *Neu1*^{hypo}*Apoe*$^{-/-}$ mice ($n = 11$) compared with *Apoe*$^{-/-}$ mice ($n = 10$). *, $p < 0.05$.

ing sialidase expression in BM-derived cells increases atherogenesis.

To determine whether sialidase expression in BM-derived cells plays a role in lipid metabolism, we measured the hepatic and serum lipid levels in the *Neu1*^{hypo}*Apoe*$^{-/-}$ mice that were transplanted with BM from *Apoe*$^{-/-}$ or *Neu1*^{hypo}*Apoe*$^{-/-}$ donors and then fed a high-fat diet for 8 weeks. We found no changes in hepatic and serum cholesterol levels in mice

Table 1

Lipid analysis in serum and liver of male *Apoe*$^{-/-}$ and *Neu1*^{hypo}*Apoe*$^{-/-}$ mice

Enzymatic assays were used to measure different lipids in the liver and serum of 7-month-old chow-fed male mice. Folch extraction was used to extract lipids from the liver, while the serum was used directly from the unfasted animals. The hepatic total and free cholesterol levels were decreased in *Neu1*^{hypo}*Apoe*$^{-/-}$ ($n = 8$) mice, while the hepatic cholesteryl ester concentration was increased (not significantly) compared with *Apoe*$^{-/-}$ mice ($n = 3$). There was a significant decrease in serum total cholesterol, free cholesterol, and cholesteryl esters in the *Neu1*^{hypo}*Apoe*$^{-/-}$ mice ($n = 8$) compared with the *Apoe*$^{-/-}$ mice ($n = 3$).

	Liver				Serum			
	Total cholesterol	Free cholesterol	Cholesteryl esters	TG	Total cholesterol	Free cholesterol	Cholesteryl esters	TG
	mg/g liver				*mM*			
Apoe$^{-/-}$	3.62 ± 0.29	3.16 ± 0.30	0.46 ± 0.13	16.98 ± 1.52	32.24 ± 2.12	14.43 ± 2.38	17.81 ± 0.69	3.32 ± 0.19
Neu1^{hypo}*Apoe*$^{-/-}$	2.22 ± 0.11[a]	1.52 ± 0.18[b]	0.70 ± 0.18	14.69 ± 1.74	14.97 ± 1.42[a]	7.45 ± 0.75[a]	7.52 ± 1.14[a]	4.38 ± 0.49

[a] Values represent the mean of biological replicates ± S.E., $p < 0.001$.
[b] Values represent the mean of biological replicates ± S.E., $p < 0.05$.

transplanted with *Neu1*^{hypo}*Apoe*$^{-/-}$ (data not shown). In addition, mice transplanted with BM from either *Apoe*$^{-/-}$ or *Neu1*^{hypo}*Apoe*$^{-/-}$ mice show no change in the levels of cholesterol or TG content of blood cells of the BM recipients (Fig. 4, *E* and *F*). The absence of an effect of BM-derived sialidase expression on the lipid metabolism in *Neu1*^{hypo}*Apoe*$^{-/-}$ mice led us to examine whether the atheroprotective effect of hypomorphic sialidase expression was due to changes in the prevalence of peripheral blood leukocytes, serum cytokines, and changes in the homing ability of leukocytes.

Peripheral blood of Neu1^{hypo}*Apoe*$^{-/-}$ *mice shows low prevalence of neutrophils and high prevalence of T cells and M2-like monocytes*

Atherosclerosis is characterized by the infiltration of monocytes, neutrophils, T lymphocytes, B cells, and NK cells into the subendothelial space. To determine whether the atheroprotective effect of hypomorphic sialidase expression in *Neu1*^{hypo}*Apoe*$^{-/-}$ mice is in part due to a significant change in the prevalence of atherogenic inflammatory cell populations in circulation, we measured the frequency of circulating CD3ϵ^{+} T cells, CD115^{hi}Ly6C$^{neg\text{-}lo}$, and CD115^{hi}Ly6C^{hi} monocytes, SSC^{hi}CD11b^{+}CD115^{lo}Ly6C^{int} neutrophils, CD19^{+} B cells, and NK1.1^{+} NK cells by flow cytometry. Peripheral blood CD3ϵ^{+} T cells were significantly increased in *Neu1*^{hypo}*Apoe*$^{-/-}$ mice compared with *Apoe*$^{-/-}$ mice (Fig. 5*A*), and within this subset, the CD3ϵ^{+} CD4^{+} T helper cells were significantly increased in the *Neu1*^{hypo}*Apoe*$^{-/-}$ mice (Fig. 5*B*). There were no differences in the CD19^{+} B cell or NK1.1^{+} NK cell populations in the *Neu1*^{hypo}*Apoe*$^{-/-}$ mice. The M2-like CD115^{hi}Ly6C$^{neg\text{-}lo}$ patrolling monocytes were more prevalent in the *Neu1*^{hypo}*Apoe*$^{-/-}$ mice, but there was no difference in the M1-like CD115^{hi}Ly6C^{hi} inflammatory monocyte population (Fig. 5*C*). A striking difference in the *Neu1*^{hypo}*Apoe*$^{-/-}$ mice was the decreased prevalence of SSC^{hi}CD11b^{+}CD115^{lo}Ly6C^{int} neutrophils. Therefore, compared with the *Apoe*$^{-/-}$ mice, the hypomorphic sialidase expression in the *Neu1*^{hypo}*Apoe*$^{-/-}$ mice significantly increased the prevalence of T helper cells and M2-like monocytes and strikingly decreased the prevalence of neutrophils within the pool of total leukocytes.

Anti-CD3ϵ stimulated Neu1^{hypo}*Apoe*$^{-/-}$ *mice show reduced levels of serum IFNγ and IL-4*

To assess if hypomorphic NEU1 provides systemic or local anti-inflammatory effects in *Apoe*$^{-/-}$ mice, we measured cytokines IL-2, IL-4, IL-10, and IFNγ from blood serum of animals either in an unstimulated state, or following an injection of anti-CD3ϵ antibody to activate secretion of cytokines from circulating T cells. In an unstimulated state, cytokines were not detected in the serum, which suggests both *Apoe*$^{-/-}$ and *Neu1*^{hypo}*Apoe*$^{-/-}$ mice do not have an active systemic inflammatory response. Following injection with anti-CD3ϵ there were significant increases in IL-2, IL-4, and IL-10 by 2 h, and IFNγ by 4 h in *Apoe*$^{-/-}$ mice. *Neu1*^{hypo}*Apoe*$^{-/-}$ mice produced 50% less IL-4 by 2 h and 90% less IFNγ by 8 h in response to T cell activation compared with *Apoe*$^{-/-}$ mice (data not shown). These observations are consistent with defective Th1 and Th2 responses when NEU1 sialidase is deficient.

Hypomorphic NEU1 expression reduces leukocyte homing

We hypothesized that the atheroprotective effect of hypomorphic sialidase expression was due in part to reduced inflammatory cell recruitment to atherosclerotic lesions. We examined how hypomorphic sialidase expression affects the binding of synthetic selectin-IgG chimeric proteins to leukocytes, which require a sialyl Lewis X ligand for binding to occur. NEU1-sialidase-dependent desialylation also increases the binding affinity of CD44 to hyaluronic acid, which is an important molecule involved in rolling and strong adhesion of leukocytes to the endothelium. Therefore, these properties led us to test whether hypomorphic sialidase expression would decrease the binding of leukocytes to hyaluronic acid.

Peripheral blood was incubated with P-selectin-human IgG, E-selectin-human IgG, or fluorescein-labeled hyaluronic acid and then with anti-CD3ϵ and anti-CD11b antibodies to identify T cells and monocytes/granulocytes, respectively. There was no difference in the P-selectin binding to CD11b^{+} cells (Fig. 6, *A* and *B*). These results did not change when the Fc block was carried out before incubation with the P-selectin-human IgG chimera. However, the CD3ϵ^{+} cells from *Neu1*^{hypo}*Apoe*$^{-/-}$ mice bound significantly less P-selectin fusion protein compared with the *Apoe*$^{-/-}$ CD3ϵ^{+} cells (Fig. 6, *C* and *D*). No difference was observed in E-selectin fusion protein binding to the cell surface of *Apoe*$^{-/-}$ and *Neu1*^{hypo}*Apoe*$^{-/-}$ CD11b^{+} or CD3ϵ^{+} cells (data not shown). Therefore, based on these data, we infer that the rolling function of T cells via P-selectin binding is hampered when NEU1 sialidase activity is reduced.

We also observed reduced hyaluronic acid binding to the cell surface of CD11b^{+} cells isolated from *Neu1*^{hypo}*Apoe*$^{-/-}$ mice compared with *Apoe*$^{-/-}$ mice (Fig. 6, *E* and *F*). CD3ϵ^{+} cells bound hyaluronic acid at two distinct levels, HA^{lo} and HA^{hi}, in *Apoe*$^{-/-}$ and *Neu1*^{hypo}*Apoe*$^{-/-}$ mice and displayed a

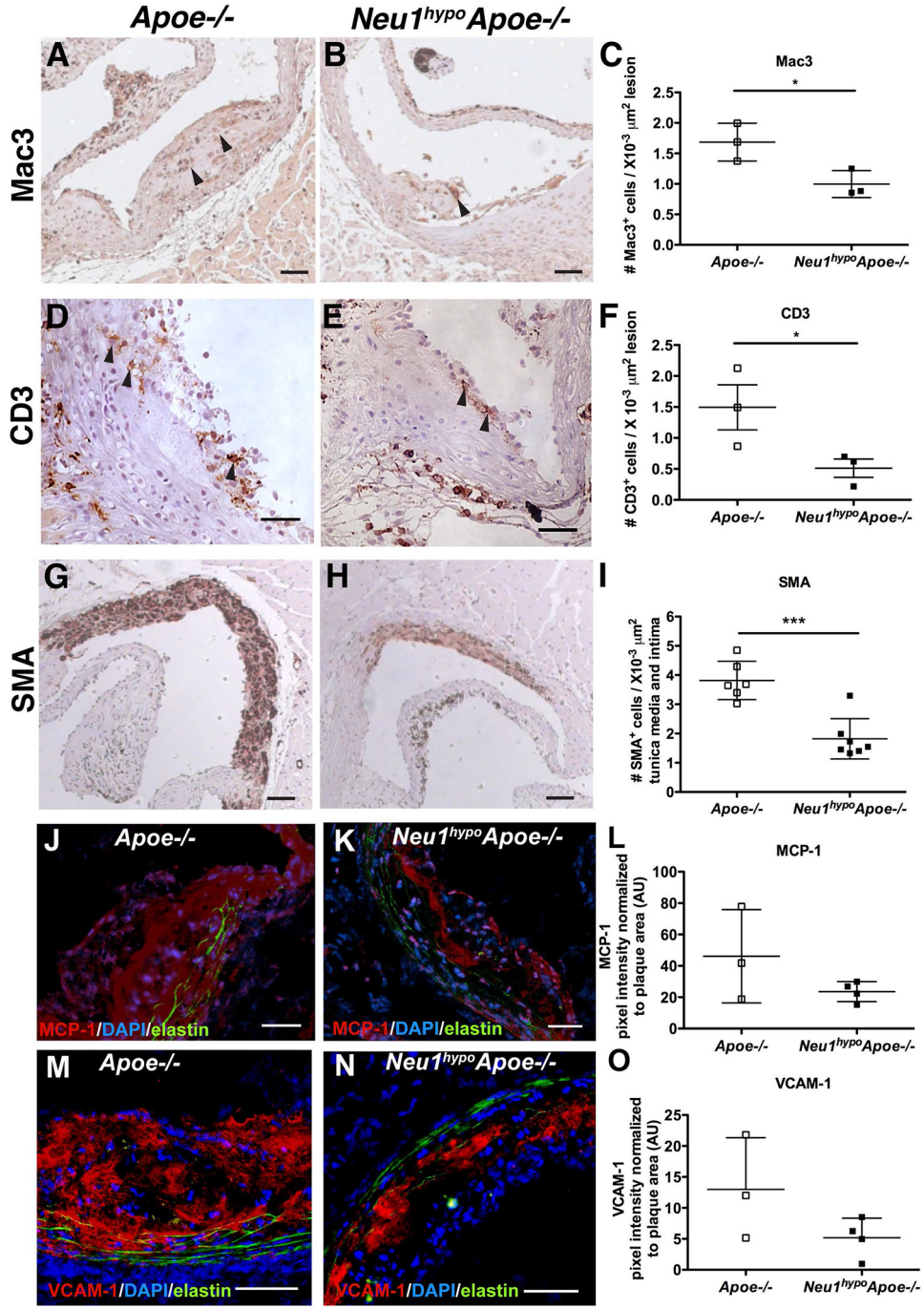

Figure 3. Assessment of cell types in the aortic sinuses of *Apoe*$^{-/-}$ and *Neu1*^{hypo}*Apoe*$^{-/-}$ mice. The infiltration of macrophages, T cells, and smooth muscle cells into the aortic sinus of 7-month-old *Apoe*$^{-/-}$ and *Neu1*^{hypo}*Apoe*$^{-/-}$ male mice was analyzed. Mac3 (*A–C*), CD3 (*D–F*), and SMA (*G–I*) were used to detect macrophages, T cells, and smooth muscle cells, respectively. Hematoxylin (*blue*) was used for nuclear staining, and representative sections are shown from male *Apoe*$^{-/-}$ and *Neu1*^{hypo}*Apoe*$^{-/-}$ mice. *Arrowheads* indicate immunoreactive Mac3^{+} and CD3^{+} cells. *Scale bars* = 50 μm. *Neu1*^{hypo}*Apoe*$^{-/-}$ male displayed a 41% reduction of Mac3^{+} cells (*C*) and a 66% reduction of CD3^{+} cells (*F*) in atherosclerotic lesions compared with controls. *I*, there was also a significant reduction of SMA^{+} cells in *Neu1*^{hypo}*Apoe*$^{-/-}$ mice compared with *Apoe*$^{-/-}$ mice. Individual data are presented with mean ± S.D. *, $p < 0.05$; ***, $p < 0.001$. *J–L*, monocyte chemoattractant protein (MCP-1) was detected in aortic sinus lesions of *Apoe*$^{-/-}$ (*J*) and *Neu1*^{hypo}*Apoe*$^{-/-}$ (*K*) mice using immunofluorescence. *Scale bars* = 50 μm. *L*, MCP-1 expression, expressed in arbitrary units (*AU*) was quantified by normalizing MCP-1 pixel fluorescence intensity to lesion area. Sialidase deficiency did not significantly alter MCP-1 expression. *M–O*, vascular cell adhesion protein 1 (VCAM-1) was detected in aortic sinus lesions of *Apoe*$^{-/-}$ ($^{-/-}$) and *Neu1*^{hypo}*Apoe*$^{-/-}$ (*N*) mice using immunofluorescence. *Scale bars* = 50 μm. *O*, VCAM-1 expression, expressed in arbitrary units (*AU*), was quantified by normalizing VCAM-1 pixel fluorescence intensity to lesion area. Sialidase deficiency did not significantly alter VCAM-1 expression. *DAPI*, 4′,6-diamidino-2-phenylindole.

significant reduction of hyaluronic acid (HA) binding in *Neu1*^{hypo}*Apoe*$^{-/-}$ mice at the HA^{lo} (Fig. 6, *G* and *H*) and HA^{hi} levels (Fig. 6, *G* and *I*). These data demonstrated that the interaction of monocytes and T cells with hyaluronic acid was impeded, which suggests that CD44 has reduced functionality on the surface of these cells.

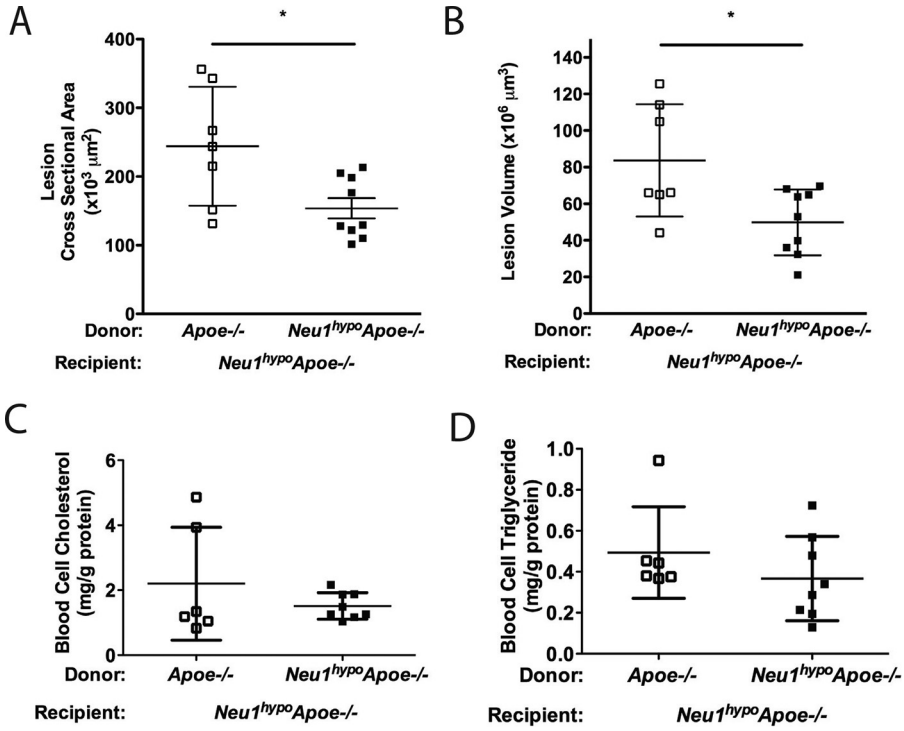

Figure 4. Atherosclerotic lesion analysis, weights, and blood cell lipids of *Neu1^{hypo}Apoe$^{-/-}$* mice transplanted with *Neu1^{hypo}Apoe$^{-/-}$* or *Apoe$^{-/-}$* BM. Aortic sinus sections of male *Neu1^{hypo}Apoe$^{-/-}$* mice transplanted with male *Apoe$^{-/-}$* BM or male *Neu1^{hypo}Apoe$^{-/-}$* BM were stained with Oil Red O and were quantified for the cross-sectional area (*A*) and volume (*B*) of atherosclerotic lesions. Transplantation of male *Apoe$^{-/-}$* BM into male *Neu1^{hypo}Apoe$^{-/-}$* mice (n = 9) resulted in increased atherosclerosis compared with male *Neu1^{hypo}Apoe$^{-/-}$* mice transplanted with male *Neu1^{hypo}Apoe$^{-/-}$* BM (n = 7). Individual data are presented with mean ± S.D. * denotes $p < 0.05$. *Scale bar* = 200 μm. *C* and *D*, blood cell lipid levels in *Neu1^{hypo}Apoe$^{-/-}$* mice transplanted with *Apoe$^{-/-}$* or *Neu1^{hypo}Apoe$^{-/-}$* BM. Blood cell cholesterol (*C*) and TG (*D*) levels in BM-transplanted mice in which male *Neu1^{hypo}Apoe$^{-/-}$* mice were transplanted with *Neu1^{hypo}Apoe$^{-/-}$* (n = 6) or *Apoe$^{-/-}$* (n = 8) BM. Blood cell cholesterol and TG levels were not significantly different between *Neu1^{hypo}Apoe$^{-/-}$* mice transplanted with *Neu1^{hypo}Apoe$^{-/-}$* BM and those transplanted with *Apoe$^{-/-}$* BM. The peripheral blood cell cholesterol and TG were determined using an enzymatic assay after extracting the blood cell lipids. Individual data are presented with mean ± S.D.

To further examine mechanisms of leukocyte homing, we used intravital microscopy and assessed the effect of hypomorphic NEU1 expression on leukocyte rolling and adhesion in the hepatic central vein (Fig. 6, *J* and *K*). Compared with WT mice, significantly more leukocytes were observed rolling along the endothelium and significantly less leukocytes were adhered to the endothelium in the *Neu1^{hypo}* mice following TNFα treatment (Fig. 6, *J* and *K*). The reduced adhesion to the endothelium was not likely due to a decrease in VCAM-1 expression as we did not observe a noticeable difference in VCAM-1 immunoreactivity in *Neu1^{hypo}Apoe$^{-/-}$* mice compared with *Apoe$^{-/-}$* mice (data not shown). Sham rescue, using adenovirus-mediated overexpression of bacterial β-Gal, did decrease the rolling behavior of leukocytes in *Neu1^{hypo}* mice (Fig. 6*J*), but this decrease did not reach WT levels. On the other hand, leukocyte adhesion to the central vein endothelium did not significantly increase when *Neu1^{hypo}* mice were infected with HD-Adβ-gal (Fig. 6*K*). Rescue of sialidase expression, using adenovirus-mediated overexpression of NEU1 (that we have previously demonstrated to rescue WT sialidase phenotype in *Neu1^{hypo}* mice (20)), did reduce the flux of rolling leukocytes to WT levels and increased the number of adherent leukocytes above WT levels (Fig. 6, *J* and *K*). These data indicate NEU1 plays an important role in both leukocyte rolling and adhesion, which are important steps leading up to leukocyte extravasation.

NEU1 activity enhances CD44-HA binding in the human THP-1 monocytic cell line

To clarify the role of NEU1 sialidase in CD44 function and its relevance in human cells, we used human THP-1 cells to specifically test the effect of NEU1 activity on the sialylation and function of CD44. In the human THP-1 monocytic cell line, the cell-surface expression of the endogenous NEU1 protein increased after 8 h LPS stimulation (Fig. 7*A*), locating NEU1 in the same compartment as its potential target CD44. Addition of the sialidase inhibitor 2-deoxy-2,3-dehydro-*N*-acetylneuraminic acid (DANA) partially attenuated the LPS-induced increase in the NEU1 expression, whereas the expression of cell-surface CD44 increased (Fig. 7, *A* and *B*). Overexpression of human NEU1 sialidase using adenovirus infection increased the proportion of THP-1 macrophages that bound HA after 10- and 30-min incubation periods (Fig. 7, *C* and *D*), compared with uninfected cells. Following the precipitation of proteins from THP-1 cell lysate samples using SNA (binds to α2,6-linked sialic acid), MALII (binds to α2,3-linked sialic acid), or peanut agglutinin (PNA) (which binds to the galactosyl (β-1,3)GalNAc that underlies the sialic acid linkage) we probed with an anti-CD44 antibody (Fig. 7*E*). In untreated cells, more CD44 was pulled down with SNA compared with MALII, which indicated CD44 had more α2,6-linked sialic acids than α2,3-linked sialic acids. Upon infection of THP-1

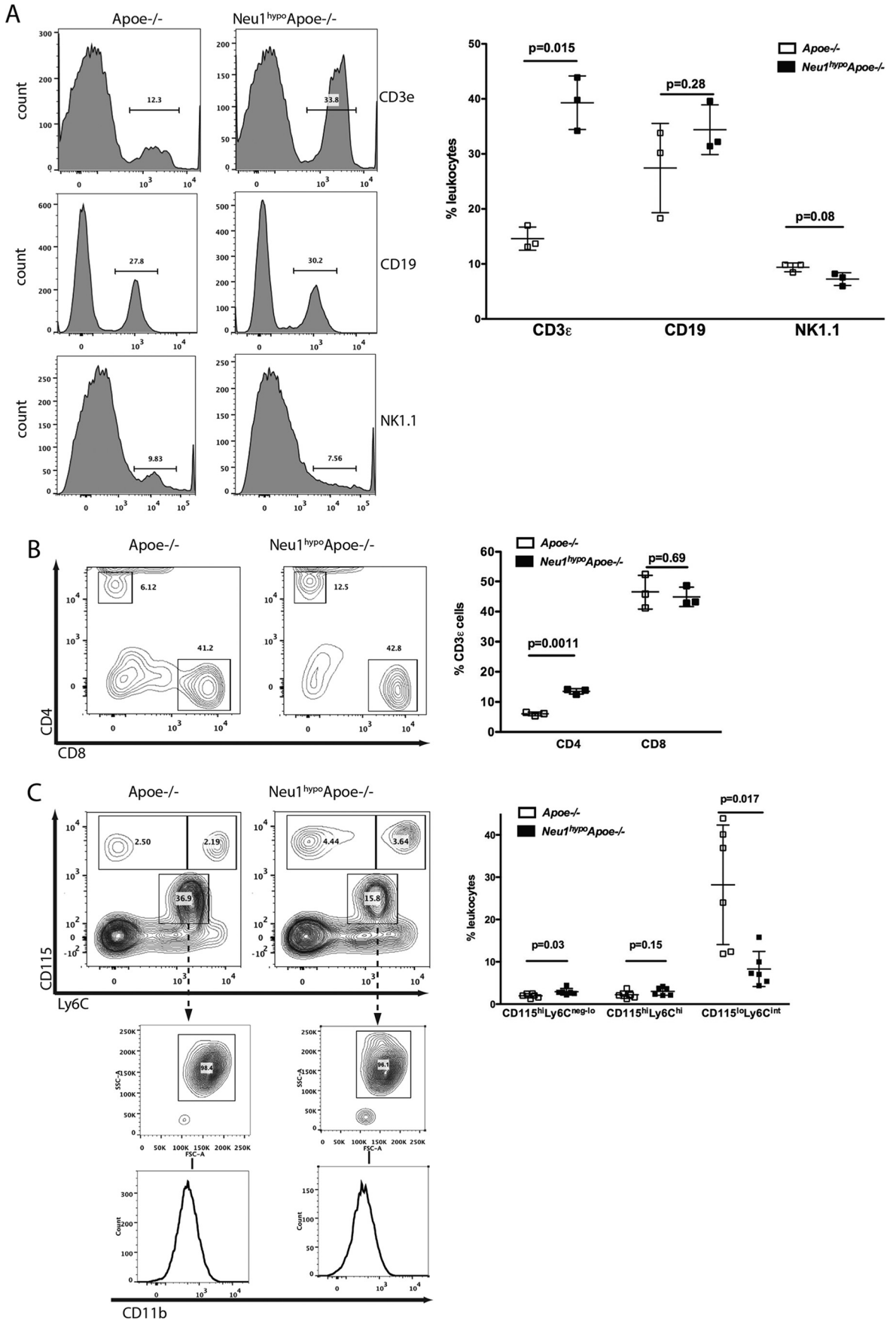
A
Apoe-/-
Neu1hypoApoe-/-
count
12.3
33.8
CD3e
27.8
30.2
CD19
9.83
7.56
NK1.1
p=0.015
p=0.28
p=0.08
Apoe-/-
Neu1hypoApoe-/-
% leukocytes
CD3ε
CD19
NK1.1
B
Apoe-/-
Neu1hypoApoe-/-
6.12
41.2
12.5
42.8
CD4
CD8
p=0.0011
p=0.69
% CD3ε cells
C
Apoe-/-
Neu1hypoApoe-/-
2.50
2.19
36.9
4.44
3.64
15.8
CD115
Ly6C
98.4
96.1
SSC-A
FSC-A
Count
CD11b
p=0.03
p=0.15
p=0.017
% leukocytes
CD115hiLy6Cneg-lo
CD115hiLy6Chi
CD115loLy6Cint

cells with adenovirus expressing NEU1 sialidase, SNA and MALII pulled down less CD44, therefore NEU1 removed sialic acids from CD44. The level of CD44 precipitated with PNA was unchanged between the untreated cells and cells infected with adenovirus-expressing sialidase, which indicated that sialidase did not affect the level of underlying galactosyl (β-1,3)GalNAc on CD44.

Pharmacological inhibition of NEU1 reduces atherosclerosis

The reduced levels of atherosclerosis observed in *Neu1*^{hypo}*Apoe*$^{-/-}$ mice suggest that the inhibition of sialidase is a therapeutic approach worth exploring to reduce atherosclerosis. Thus, we selected a mammalian sialidase inhibitor, DANA (25), to investigate whether the chemical inhibition of sialidase can reduce atherosclerosis in male *Apoe*$^{-/-}$ mice. After administration of DANA in male *Apoe*$^{-/-}$ mice for 6 weeks, we observed a significant reduction in hepatic total cholesterol, free cholesterol, and cholesteryl esters when compared with control mice (Fig. 8*A*). Aortic sinus lesions from the DANA-treated male *Apoe*$^{-/-}$ mice were significantly smaller in area and volume compared with saline-treated control mice (Fig. 8, *B–E*). These results indicate that sialidase inhibition by DANA is effective in halting atherosclerotic lesion progression at the aortic sinus. We also performed a similar control experiment using oseltamivir (also known as Tamiflu), a specific inhibitor of influenza virus sialidase, which does not effectively inhibit mammalian sialidases. Male *Apoe*$^{-/-}$ mice were treated with oseltamivir for 6 weeks, followed by analysis of atherosclerosis. We found no significant difference in the atherosclerotic-lesion area or volume of the aortic sinus after oseltamivir treatment, showing that oseltamivir did not reduce the atherosclerotic plaque formation in male *Apoe*$^{-/-}$ mice (data not shown). The mammalian sialidase inhibitor, DANA is therefore effective in reducing atherosclerosis in mice.

Discussion

NEU1 sialidase is involved in the development of inflammatory responses, including the activation of macrophages, neutrophils, and T cells (2–6). In addition, NEU1 is implicated in the removal of sialic acid from leukocyte cell-surface adhesion molecules (14, 15, 26), and signaling in the Toll-like receptor 4 (TLR4) pathway (27, 28). Furthermore, the modification of sialic acids on apolipoproteins can affect lipoprotein metabolism (29–31), and lower LDL sialylation levels are associated with coronary heart disease in humans (18). We have shown that hypomorphic sialidase expression can affect lipoprotein metabolism in the mouse (20). Recently, an animal model with partial deficiency in cathepsin A was used to illustrate that elastin degradation products promote atherosclerosis through the action of the cathepsin A-GAL-NEU1 complex signaling pathway (32). However, no current *in vivo* studies have directly assessed the sole impact of sialidase expression or activity on atherosclerosis and the mechanisms of disease progression. In this report, we demonstrate that hypomorphic NEU1 sialidase expression or inhibition of sialidase both attenuate atherosclerosis in *Apoe*$^{-/-}$ mice. The mechanism underlying the protective effect of hypomorphic sialidase expression includes reduced cholesterol levels in VLDL- and LDL-sized particles and reduced immune-cell infiltration into lesions. BM-derived NEU1 sialidase does not contribute to lipoprotein metabolism, but does increase lesion size, suggesting that sialidase plays an important role in the inflammatory component of atherosclerosis. This is supported by our finding that hypomorphic sialidase expression decreased the proportion of circulating neutrophils in *Neu1*^{hypo}*Apoe*$^{-/-}$ mice and reduced the potential of T cells and monocytes/neutrophils to interact with the cell adhesion molecules that are normally presented by inflamed endothelium.

Neu1^{hypo}*Apoe*$^{-/-}$ mice have lower levels of both total hepatic cholesterol and free hepatic cholesterol compared with *Apoe*$^{-/-}$ mice. These differences support the hypothesis that hypomorphic sialidase expression modulates the uptake, storage, and metabolism of cholesterol in the liver, and this modulation could be the contributing force behind the reduction in serum lipoprotein. VLDL-TG production is also decreased in these mice and is most likely due to the reduced lipid content of the liver, because we have also observed lower VLDL production in hypomorphic sialidase mice on a C57BL/6 background (20). We must note that due to age differences in the mice used for the regular chow diet (7 months old) compared with the high-fat diet (2 months old), we observed lower VLDL and IDL/LDL-associated cholesterol in the high-fat diet fed mice. *Neu1*^{hypo}*Apoe*$^{-/-}$ mice also exhibit drastically lower levels of total serum cholesterol, which lowers the risk for atherosclerosis and further supports the notion that hypomorphic sialidase expression can alter the entire lipid metabolism profile of the mouse. Overall, we postulate that lower hepatic lipids cause lower VLDL-TG secretion and result in less serum LDL cholesterol.

The comparison of the quantity of SMA$^+$ smooth muscle cells within the wall of the aortic sinus reveals a role for NEU1 sialidase in the maintenance of smooth muscle cells. The reduced smooth muscle cell content in the aortic sinus of *Neu1*^{hypo}*Apoe*$^{-/-}$ compared with *Apoe*$^{-/-}$ mice is consistent with reports that NEU1-dependent desialylation increases smooth muscle cell proliferation (33). However, the decreased tunica media and intima smooth muscle content of *Neu1*^{hypo}*Apoe*$^{-/-}$ mice may also be a result of reduced Th1 cytokine secretion from the lower number of T cells and macrophages in the lesions. The reduction of macrophages in the lesion also correlates with a substantial decrease in the relative prevalence of SSC^{hi}CD11b$^+$CD115^{lo}Ly6C^{int} neutrophils/gran-

Figure 5. Peripheral blood immunophenotypes in male *Apoe*$^{-/-}$ and *Neu1*^{hypo}*Apoe*$^{-/-}$ mice. Samples were treated with ACK lysis buffer, blocked with CD16/CD32 antibody, stained with directly conjugated antibodies for the cell-surface markers, fixed, and run on an LSR II flow cytometer. *A,* proportions of CD3ϵ^+ T cells, CD19$^+$ B cells, and NK1.1$^+$ NK cells in peripheral blood. The male *Neu1*^{hypo}*Apoe*$^{-/-}$ mice displayed increased CD3ϵ^+ T cells but slightly reduced NK1.1$^+$ NK cells. *B,* proportions of CD4$^+$ T helper lymphocytes and CD8$^+$ cytotoxic T lymphocytes subsets in the CD3ϵ^+ gate. The male *Neu1*^{hypo}*Apoe*$^{-/-}$ mice had a significantly greater prevalence of CD4$^+$ T helper lymphocytes. *C,* prevalence of CD115^{hi}Ly6C$^{neg\text{-}lo}$ patrolling monocytes, CD115^{hi}Ly6C^{hi} inflammatory monocytes, and SSC^{hi}CD11b$^+$CD115^{lo}Ly6C^{int} neutrophils. The male *Neu1*^{hypo}*Apoe*$^{-/-}$ mice exhibited subtle increases in the monocyte populations and a striking decrease in the neutrophil prevalence. Individual data are presented with mean frequency ± S.D. presented in each graph (n = 3–6 for each group).

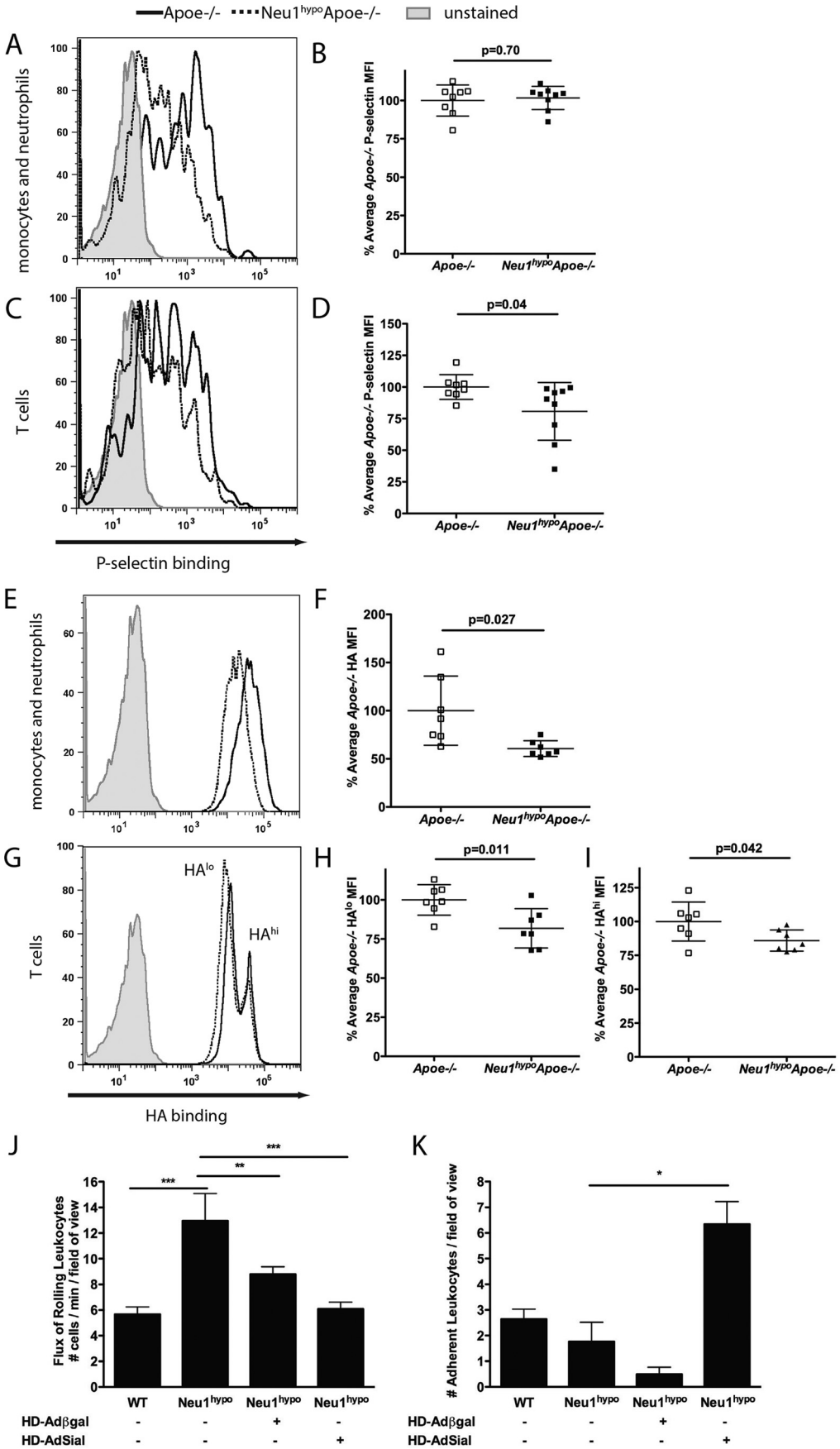
Apoe-/-
Neu1hypoApoe-/-
unstained
A
monocytes and neutrophils
B
p=0.70
% Average Apoe-/- P-selectin MFI
Apoe-/-
Neu1hypoApoe-/-
C
T cells
P-selectin binding
D
p=0.04
% Average Apoe-/- P-selectin MFI
Apoe-/-
Neu1hypoApoe-/-
E
monocytes and neutrophils
F
p=0.027
% Average Apoe-/- HA MFI
Apoe-/-
Neu1hypoApoe-/-
G
T cells
HAlo
HAhi
HA binding
H
p=0.011
% Average Apoe-/- HAlo MFI
Apoe-/-
Neu1hypoApoe-/-
I
p=0.042
% Average Apoe-/- HAhi MFI
Apoe-/-
Neu1hypoApoe-/-
J
Flux of Rolling Leukocytes
cells / min / field of view
WT
Neu1hypo
Neu1hypo
Neu1hypo
HD-Adβgal - - + -
HD-AdSial - - - +
K
Adherent Leukocytes / field of view
WT
Neu1hypo
Neu1hypo
Neu1hypo
HD-Adβgal - - + -
HD-AdSial - - - +

ulocytes in the peripheral blood. Neutrophils typically exacerbate atherosclerosis by producing myeloperoxidase and lipoxygenase enzymes and by promoting oxidative stress (reviewed in Ref. 34). Indeed, a direct correlation between the number of circulating neutrophils and the atherosclerotic lesion size has been demonstrated in *Apoe*$^{-/-}$ mice (35). Neutrophil depletion impairs the development of lesion formation in the mouse aortic sinus, including reduced macrophage content (1). Thus, hypomorphic sialidase expression reduces the relative prevalence of peripheral blood neutrophils, which in turn contribute to the reduction of atherosclerotic lesion formation in *Neu1*^{hypo}*Apoe*$^{-/-}$ mice. Sialidase is heavily involved in the desialylation of cell-surface cell adhesion molecules and plays a role in intercellular adhesion in our mouse model by influencing the recruitment and infiltration of immune cells into atherosclerotic lesions. We present evidence that hypomorphic sialidase expression reduces T cell recruitment to lesions. This evidence includes an increase in the prevalence of peripheral blood CD4$^+$ T cells, along with a reduction in the accumulation of T cells within the lesions of *Neu1*^{hypo}*Apoe*$^{-/-}$ mice. Interestingly, the increased prevalence of circulating CD4$^+$ T cells does not reflect the compromised IFNγ production in response to anti-CD3 stimulation, but is likely a consequence of the impaired T cell tissue infiltration, *e.g.* into the atherosclerotic lesion. Furthermore, we have direct evidence that *Neu1*^{hypo} mice have increased leukocyte rolling and decreased leukocyte adhesion along TNFα-activated endothelium in the hepatic circulation. This leukocyte behavior can be reversed by rescue of NEU1 sialidase expression in *Neu1*^{hypo} mice, which reduces the flux of rolling leukocytes within circulation and increases the number of leukocytes that adhere to the endothelium.

Synchronized expression of selectins and their ligands are required for leukocyte-endothelium interactions (*i.e.* rolling and adhesion). Inflammation-activated endothelial cells express P-selectin and E-selectin, which bind to leukocyte PSGL-1, CD44, and CD34 via their sialyl Lewis X motif (reviewed in Ref. 36). These low-affinity adhesion interactions initiate an intracellular response and activate integrins expression (VLA-4 and LFA-1) on leukocytes, permitting high-affinity adhesion of the leukocytes to the endothelium and leukocyte extravasation (36). Because sialidase deficiency is associated with hypersialylation of cell-surface molecules and because selectin ligands require a sialylated motif, we hypothesize that the reduction of P-selectin binding observed in T cells is associated with hypersialylation of motifs or that the presentation of selectin ligands was reduced. As a component of the extracellular matrix, hyaluronic acid acts as a ligand for CD44 with higher binding affinity toward desialylated CD44 (15, 26, 37). Reduced hyaluronic acid binding on CD11b$^+$ cells in the *Neu1*^{hypo}*Apoe*$^{-/-}$ mice also suggests that NEU1-dependent removal of CD44 sialic acids is important for increased binding to occur. Indeed, we clearly link the Neu1-dependent removal of α2,3- and α2,6-linked sialic acids from CD44 with an increased proportion of THP-1 cells that bound HA. This deficiency would reduce the migratory and extravasation potential of peripheral blood monocytes, thereby reducing their contribution to atherosclerotic lesion formation in *Neu1*^{hypo}*Apoe*$^{-/-}$ mice. Therefore, hypomorphic sialidase expression causes reduced leukocyte recruitment and homing to the endothelium by negatively affecting the binding of cell adhesion molecules.

By utilizing bone marrow transplantation (38), we have shown that NEU1 expression in BM-derived cells does not alter the lipid metabolism in *Neu1*^{hypo}*Apoe*$^{-/-}$ mice. This finding is demonstrated by the absence of a difference in the serum and hepatic lipid levels between *Neu1*^{hypo}*Apoe*$^{-/-}$ mice transplanted with *Apoe*$^{-/-}$ or *Neu1*^{hypo}*Apoe*$^{-/-}$ BM. Therefore, the altered hepatic and serum lipids we have observed in *Neu1*^{hypo}*Apoe*$^{-/-}$ mice compared with *ApoE*$^{-/-}$ mice are not due to hypomorphic sialidase expression in BM-derived cells but are more likely due to altered sialidase expression in the liver. These data suggest that leukocytes are important contributors in the development of atherosclerosis because leukocyte sialidase deficiency appears to account for the majority of the atherogenic effect in *Neu1*^{hypo}*Apoe*$^{-/-}$ mice. We cannot, however, rule out the possibility that altered lipoprotein metabolism may also contribute and further research is required to test if this is the case. The inflammatory response likely works in synergy with lipoprotein metabolism in this model of atherosclerosis. These crucial processes both underlie disease progression and exhibit significant cross-talk and dependence (39, 40). The changes we observed in neutrophil frequency in male *Neu1*^{hypo}*Apoe*$^{-/-}$ mice may be a result of differences in serum cholesterol levels. Mechanistically, the granulocyte-macrophage colony-stimulating factor receptor on myeloid progenitors is up-regulated in response to higher cellular cholesterol, and it is linked to hyperlipidemia-induced neutrophilia (41). This mechanism would make our model another example of the harmonious balance between immune cells and lipoprotein metabolism in modulating atherogenesis.

This novel role for sialidase in atherogenesis indicates its potential as a therapeutic target. The sialidase inhibitor, DANA, is a modified form of sialic acid, *i.e.* 2,3-dehydro-2-

Figure 6. P-selectin and hyaluronic acid-binding assay in CD11b$^+$ and CD3ϵ^+ peripheral blood subsets in male *Apoe*$^{-/-}$ and *Neu1*^{hypo}*Apoe*$^{-/-}$ mice. Hypomorphic sialidase *Apoe*$^{-/-}$ peripheral blood displayed no difference in P-selectin binding in the CD11b$^+$ (*A* and *B*) subsets ($p = 0.70$), but a significant reduction of P-selectin binding in the CD3ϵ^+ (*C* and *D*) subsets was observed ($p = 0.04$). Peripheral blood was incubated with 4 μg of P-selectin-human IgG chimera for 1 h and then incubated with anti-human IgG-AF488, anti-CD11b-APC, and anti-CD3ϵ-Pacific Blue. Samples were analyzed on an LSR II, $n = 8$ *Apoe*$^{-/-}$ and $n = 9$ *Neu1*^{hypo}*Apoe*$^{-/-}$; the data were analyzed using a two-tailed Student's *t* test. *E–I*, HA binding on *Apoe*$^{-/-}$ and *Neu1*^{hypo}*Apoe*$^{-/-}$ peripheral blood. *E* and *F*, the CD11b$^+$ monocytes and neutrophils exhibited significantly reduced hyaluronic acid binding ($p = 0.027$), whereas the CD3ϵ^+ cells (*G–I*) displayed two distinct populations that bound hyaluronic acid at different amounts, HA^{lo} (*H*) and HA^{hi} (*I*), and showed significantly reduced hyaluronic acid binding in *Neu1*^{hypo}*Apoe*$^{-/-}$ cells ($p = 0.042$ for the HA^{hi} group and $p = 0.011$ for the HA^{lo} group, two-tailed Student's *t* test). *J* and *K*, leukocyte recruitment in the hepatic central vein of WT and *Neu1*^{hypo} animals was analyzed by intravital microscopy following sham treatment with helper-dependent adenovirus expressing bacterial β-Gal (HD-Adβ-gal), or rescue with helper-dependent adenovirus expressing NEU1 sialdiase (HD-AdSial), and TNFα treatment to activate leukocyte extravasation. *J*, the flux of leukocytes rolling along the endothelium was quantified as the number of cells per min per field of view. Hypomorphic sialidase mice showed a significant increase in the flux of rolling leukocytes, which was reduced following rescue with HD-AdSial. *K*, the number of leukocytes adherent to the endothelium was quantified per field of view. The number of firm cell adhesion events was significantly impeded with hypomorphic NEU1 sialidase expression, and significantly increased after HD-AdSial-mediated overexpression. *, $p < 0.05$; **, $p < 0.01$; ***, $p < 0.001$.

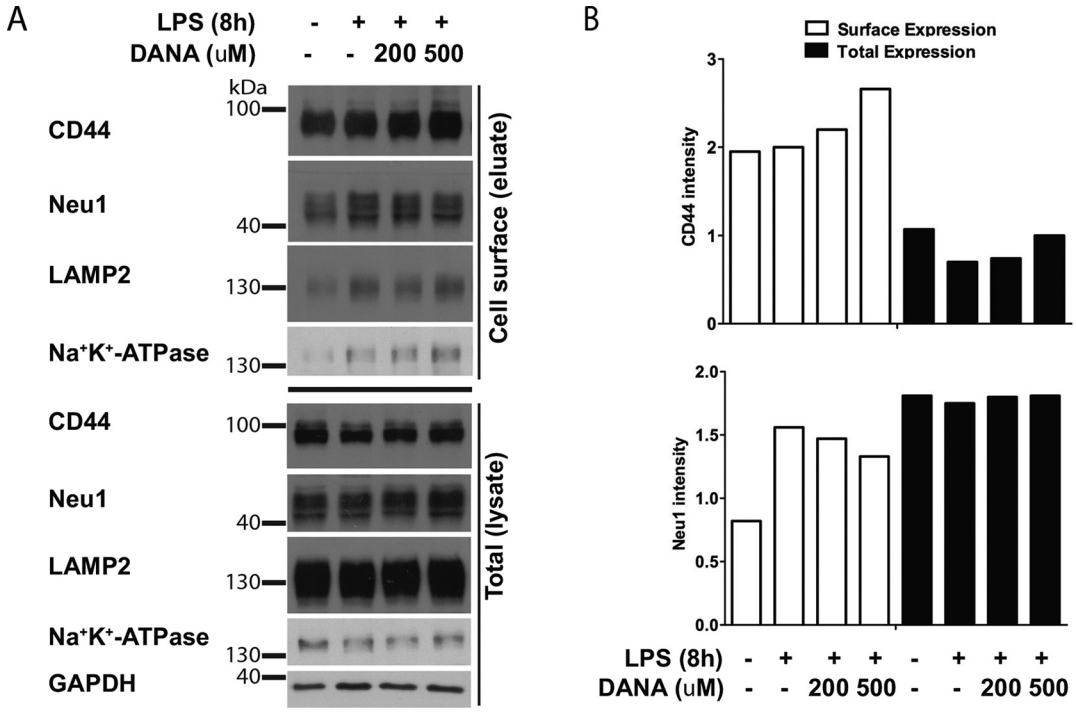
A
LPS (8h) - + + +
DANA (uM) - - 200 500
kDa
CD44
Neu1
LAMP2
Na+K+-ATPase
Cell surface (eluate)
CD44
Neu1
LAMP2
Na+K+-ATPase
GAPDH
Total (lysate)
B
Surface Expression
Total Expression
CD44 intensity
Neu1 intensity
LPS (8h) - + + + - + + +
DANA (uM) - - 200 500 - - 200 500

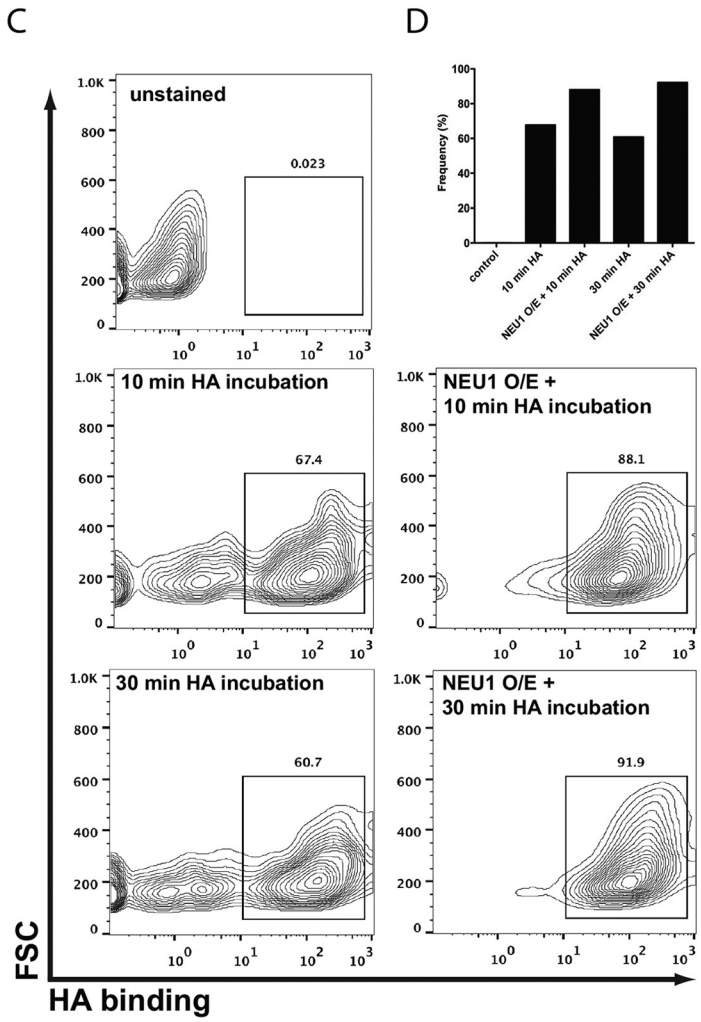
C
unstained
0.023
10 min HA incubation
67.4
NEU1 O/E +
10 min HA incubation
88.1
30 min HA incubation
60.7
NEU1 O/E +
30 min HA incubation
91.9
FSC
HA binding
D
Frequency (%)
control
10 min HA
NEU1 O/E + 10 min HA
30 min HA
NEU1 O/E + 30 min HA

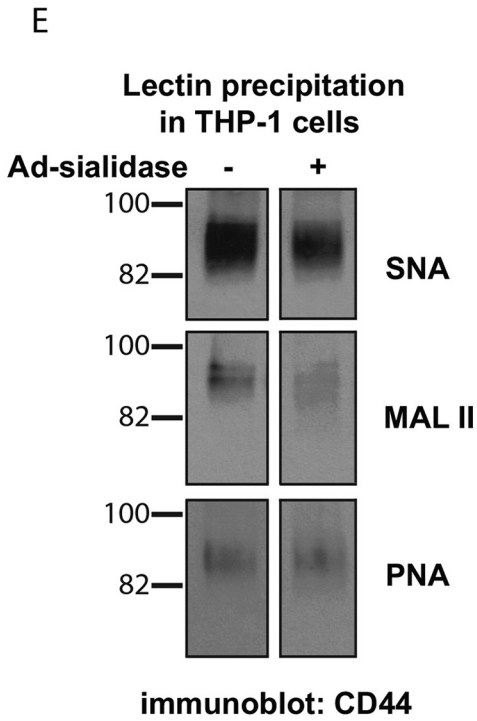
E
Lectin precipitation
in THP-1 cells
Ad-sialidase - +
SNA
MAL II
PNA
immunoblot: CD44

A

	Hepatic Total Cholesterol (mg/g liver)	Hepatic Free Cholesterol (mg/g liver)	Hepatic Cholesteryl Esters (mg/g liver)	Hepatic Triglyceride (mg/g liver)
Saline	4.48±0.07	3.82±0.21	0.66±0.25	10.07±1.77
DANA	3.44±0.20*	1.82±0.32*	1.62±0.35*	7.02±0.62

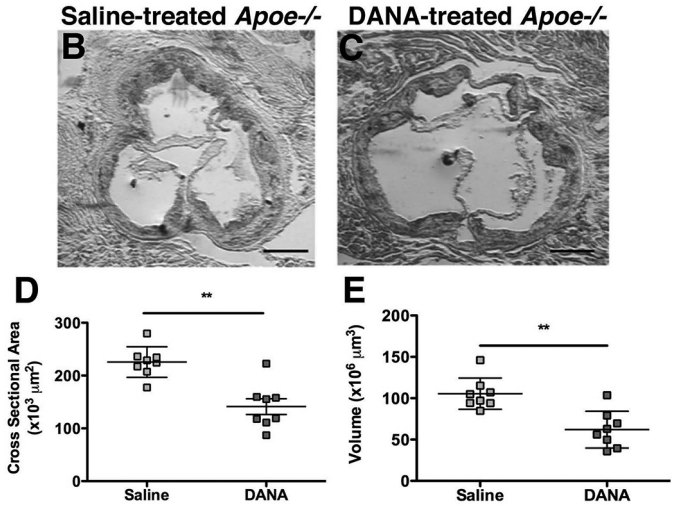

Figure 8. Hepatic lipids levels and atherosclerotic lesion analysis in male *Apoe*$^{-/-}$ mice treated with sialidase inhibitors. *A,* hepatic total cholesterol, free cholesterol, cholesteryl esters, and TG concentrations were compared among saline-treated *Apoe*$^{-/-}$ mice ($n = 8$) and DANA-treated *Apoe*$^{-/-}$ mice ($n = 8$). DANA-treated *Apoe*$^{-/-}$ mice showed a trend toward a reduction in TG and a significant increase in cholesteryl esters compared with saline-treated *Apoe*$^{-/-}$ mice. The mice were fasted overnight prior to sample collection, and the values represent individual data with mean ± S.D. *B* and *C,* cross-sections of the aortic sinuses from saline-treated *Apoe*$^{-/-}$ (*B*) ($n = 8$), and DANA-treated *Apoe*$^{-/-}$ (*C*) mice ($n = 8$). Sections were stained with Oil Red O for neutral lipids and counterstained with hematoxylin for nuclei. The mice were 8 months of age at the beginning of treatment. DANA and saline were then administered for 6 weeks, and all mice were fed a regular chow diet. The atherosclerotic lesion area (*D*) and volume (*E*) were significantly reduced in DANA-treated male *Apoe*$^{-/-}$ mice compared with saline-treated male *Apoe*$^{-/-}$ mice. *Scale bar* = 200 μm. Individual data are presented with mean ± S.D. *, $p < 0.05$; and **, $p < 0.01$.

deoxy-*N*-acetylneuraminic acid. DANA inhibits sialidases by binding to the catalytic site and acting as a transition state analog (25). We utilized DANA to determine the effects of sialidase inhibition on atherosclerosis in *Apoe*$^{-/-}$ mice because of its specificity for sialidase enzymes and its cell-impermeability that limits its toxicity (25, 42, 43). Treatment of *Apoe*$^{-/-}$ mice with DANA significantly reduced atherogenesis, indicating that chemical sialidase inhibition is sufficient for atheroprotection. DANA treatment produced protection against atherosclerosis, accompanied with a slight reduction in hepatic lipid content; however, one would expect immune cell recruitment and homing to be significantly reduced as well. Interestingly, DANA inhibited the binding of hyaluronic acid to THP-1 monocytic cells, which indicates sialidase inhibition will reduce monocyte CD44-dependent recruitment to the endothelium. This effect is not surprising because DANA treatment would preserve the sialic acid content of leukocyte and endothelium cell adhesion molecules and thus interfere with leukocyte infiltration into the plaque. We also observed that DANA reduces the cell-surface expression of NEU1 in THP-1 monocytic cells, which could be a consequence of inhibiting low levels of steady-state cell-surface NEU1, which normally induces the increase of cell-surface NEU1 after LPS treatment of THP-1 cells (*i.e.* cell-surface NEU-1-induced trafficking of intracellular pools of NEU1 to the cell surface). Considering our data, and notwithstanding the fact that the *Apoe*$^{-/-}$ mouse does not show acute myocardial infarction, inhibiting sialidase with DANA can serve to effectively reduce atherosclerosis in *Apoe*$^{-/-}$ mice, further adding to the hypothesis that sialidase plays a pivotal role in atherogenesis. To be an effective anti-atherogenic therapy in humans, the quick systemic clearance and excretion of DANA (44) has to be countered by a slow and a more localized release of the drug, potentially by using a drug-releasing stent. Alternatively, a derivative of DANA with a longer half-life would be worthwhile to test. Additionally, the anti-inflammatory effects of DANA need to be further investigated to ensure maximal anti-atherogenic effects.

In this report, we provide *in vivo* evidence that hypomorphic sialidase expression reduces serum cholesterol levels and atherosclerosis in *Apoe*$^{-/-}$ mice. Modification of the hepatic lipid metabolism, a reduced proportion of circulating neutrophils, and altered adhesion molecule function on leukocytes all contribute significantly to reducing atherosclerosis in *Neu1*^{hypo}*Apoe*$^{-/-}$ mice. Reducing sialidase activity in BM-derived cells is sufficient to reduce atherosclerosis in *Neu1*^{hypo}*Apoe*$^{-/-}$ mice, independently of the hepatic and serum lipids levels. In addition to our evidence that a genetic model of reduced sialidase expression is atheroprotective, we conclude that sialidase inhibition using DANA also reduces atherosclerosis. Our study presents evidence that hypomorphic sialidase expression can protect against the atherogenic effects of ApoE deficiency in mice and that sialidase inhibition should be further tested as a potential treatment for atherosclerosis in humans.

Experimental procedures

Generation of mice

Neu1^{hypo} mice harbor a mutation that reduces enzymatic activity significantly and mice were backcrossed to a B57Bl6 background as described previously (20). The presence of the regulatory mutation (−519G → A) within the neu1 promoter was confirmed by PCR using DNA extracted from tail biopsies.

Figure 7. NEU1 desialylation of CD44 leads to an increased proportion of THP-1 cells that bind hyaluronic acid. *A,* CD44 and NEU1 protein expression at the cell surface in untreated cells, 8-h LPS, 8-h LPS + 200 μM DANA, or 8-h LPS + 500 μM DANA. Controls included Na^+-K^+-ATPase for cell-surface protein, LAMP2 for lysosomal protein, and GAPDH for cytosolic protein. Cell-surface proteins were biotinylated, purified, and blotted for the various antibodies. *B,* quantification of CD44 and NEU1 expression at the cell-surface *versus* total cell expression. *C* and *D,* THP-1 cells infected with adenovirus-expressing human NEU1 sialidase (NEU1 O/E = NEU1 overexpression) bound more HA compared with uninfected cells. Unstained cells were used as a control. The proportion of cells binding HA was measured using the *box* indicated in *C*. *E,* sialylation of CD44 was examined following infection of THP-1 cells with adenovirus-expressing human NEU1 sialidase, by immunoprecipitation of protein using *S. nigra* (SNA) lectin (α2,6-linked sialic acid levels), *M. amurensis* lectin II (MALII) lectin (α2,3-linked sialic acid), or PNA lectin (binds underlying galactosyl (α-1,3) GalNAc structure), followed by probing lectin-precipitated protein with anti-CD44 antibody.

The following primers were used for the PCR: 5′-ATC CCT GTC CAG GAA CTG GT-3′ and 5′-CTT AAG GGC ATT GGG GTC AT-3′, synthesized by Mobix facility at McMaster University. PCR (40 cycles) was performed with denaturing temperature at 94 °C for 2 min, annealing temperature at 60 °C for 30 s, and elongation temperature at 72 °C for 30 s. PCR products were digested with MspA1I (New England BioLab), which serves as a genetic diagnostic as it only cleaves the PCR product carrying the B6.SM mutation. To generate $Neu1^{hypo}Apoe^{-/-}$ mice, $Neu1^{hypo}$ mice were crossed four times with $Apoe^{-/-}$ mice, which are on a C57BL/6 background. $Neu1^{hypo}Apoe^{-/-}$ and age- and gender-matched $Apoe^{-/-}$ controls were used for the atherosclerosis studies. Mice were permitted free access to a standard chow diet and water, unless otherwise stated. All procedures were approved by the McMaster University Animal Research Ethics Board and were in accordance with the policies of the Canadian Council on Animal Care. In addition, all studies conducted abide by the Declaration of Helsinki principles.

Treatment of mice

Male $Apoe^{-/-}$ mice and $Neu1^{hypo}Apoe^{-/-}$ mice were fed a regular chow diet and spontaneous atherosclerosis was quantified at 7 months of age. These animals were also used for immunohistochemistry studies. For accelerated atherosclerosis, 1-month-old male $Apoe^{-/-}$ and $Neu1^{hypo}Apoe^{-/-}$ mice were fed a Western style diet that contained 21% butterfat and 0.15% cholesterol with 1% safflower oil (modified Stanford University, Dyets Inc., Bethlehem, PA, catalogue number 112286). Mice were fed a Western style high-fat diet for 1 month and harvested at 2 months of age. For sialidase inhibition studies, male $Apoe^{-/-}$ mice (8 months old) were administered a sialidase inhibitor, DANA, or saline using mini-osmotic pumps (Alzet osmotic pump, Model 2004, DURECT Corp., Cupertino, CA). DANA (Toronto Research Chemicals, Toronto, ON) was dispensed at a rate of 0.06 μg/h for 6 weeks. The treatment groups were sacrificed at 9.5 months of age and atherosclerosis was quantified. For the oseltamivir-treated $Apoe^{-/-}$ mice, oseltamivir (Roche Applied Science, Mississauga, ON, Canada), was dissolved in drinking water and was administered daily to 8-month-old male $Apoe^{-/-}$ mice for 6 weeks before atherosclerosis was quantified.

Collection of blood and tissues

Mice were anesthetized with ketamine/xylazine. Blood was obtained by cardiac puncture. Serum was prepared by collecting the supernatant after centrifugation of whole blood for 5 min at 15,000 rpm using serum collection tubes (Sarstedt, Montreal, QC). Animals were perfused with phosphate-buffered saline (PBS) through the left ventricle of the heart and drained via the right atrium. Hearts were immersed in Krebs/Henseleit solution followed by 4% formaldehyde. Livers were snap frozen in liquid nitrogen and stored in −80 °C before lipid analysis.

Serum lipid and lipoprotein analysis

Serum lipids were fractionated by gel filtration-FPLC using an AKTA system with a Superose 6 10/300 GL column (GE Healthcare Life Sciences, Baie d'Urfe, QC). Enzymatic assay kits were used to measure total and free cholesterol levels (Infinity™ Cholesterol Liquid Stable Reagent, Thermo Fisher Scientific, Burlington, ON; Free Cholesterol E Reagent, Wako Diagnostics, Richmond, VA). The concentration of cholesterol esters was calculated by subtracting the free cholesterol concentration from the total cholesterol concentration. Triglyceride concentration was also measured using an enzymatic assay (L-type Triglyceride H Reagents 1 and 2, Wako Diagnostics).

Hepatic and blood cell lipid analyses

Prior to analysis of lipids using the enzymatic assays described above, lipids were isolated from liver or blood cells. Liver or blood cell homogenates were prepared by homogenizing 150 mg of liver or blood cell pellet in 1 ml of TNES (10 mM Tris, pH 7.5, 400 mM NaCl, 100 mM EDTA, 0.6% SDS), and lipids were isolated by the Folch method, as previously described (20, 45). Blood cell lipid analysis was normalized to sample protein concentration after performing Bradford protein assays.

In vivo hepatic VLDL-TG secretion

Male $Apoe^{-/-}$ and $Neu1^{hypo}Apoe^{-/-}$ mice (3 months of age) were used for hepatic VLDL-TG production studies and were fasted overnight before injection of 500 mg/kg of Triton WR1339 (in 0.9% sterile NaCl, Sigma) to inhibit plasma lipoprotein lipase. To determine the rate of hepatic TG secretion after the injection, blood was collected hourly at baseline (0 h, prior to injection) and at 1, 2, 3, and 4 h after Triton WR1339 injection (46–48). Serum was separated from whole blood using serum collection tubes, as described above. Serum TG was measured by enzymatic methods, and VLDL-TG production rates were obtained from the regression lines when graphing the VLDL-TG concentration *versus* time (hours).

Analysis of atherosclerotic lesions

Hearts were frozen in Shandon™ Cryomatrix™ embedding resin (Thermo Fisher Scientific), and serial 10-μm sections were cut using a Shandon cryostat (Thermo Fisher Scientific). Sections were immersed in Oil Red O (Sigma) to stain for neutral lipids and hematoxylin to counterstain nuclei, and atherosclerosis was quantified as the total cross-sectional area of atherosclerotic lesion (including the acellular atherosclerotic core) in each given section. The volumes of the aortic lesions were calculated by measuring lesion areas in representative sections separated by 100 μm (along the total length of the lesion), and the volume was approximated by the sum of each representative lesion area × 100 μm for the total length of the lesion to give the volume in μm^3. *En face* aorta lesion staining with Sudan IV (Sigma) was performed as previously described by Covey *et al.* (49).

Immunohistochemistry

Paraffin sections of the aortic root or liver were de-paraffinized in xylene and endogenous peroxidases were blocked with 1.7% H_2O_2 in methanol. Heat-induced antigen retrieval was performed in citrate buffer, pH 6.0, for NEU1, Mac3, and CD3 immunohistochemistry. Sections were blocked with 5% normal goat or rabbit serum and stained with polyclonal rabbit

anti-NEU1 sialidase (1:200, Rockland Immunochemicals Inc., Gilbertsville, PA), monoclonal rat anti-Mac3 (1:500, BD Pharmingen, Mississauga, ON), polyclonal rabbit anti-CD3 (1:200, Dako, Burlington, ON), monoclonal mouse anti-SMA clone 1A4 (1:200, Neomakers Inc., Fremont, CA), or goat anti-VCAM-1 (1:20, AF643, R&D Systems, Minneapolis, MN), followed by detection with goat anti-rabbit IgG, goat anti-rat IgG, or rabbit anti-goat IgG-biotinylated antibody and avidin-biotin HRP (1:500, Vector Laboratories, Burlington, ON) (50). For SMA detection, an anti-mouse Envision-HRP secondary antibody (Dako) was used. Immunoreactivity was visualized using NovaRED (Vector Laboratories) or diaminobenzidine (Sigma), sections were counterstained with hematoxylin (Sigma), and slides were mounted with Permount (Thermo Fisher Scientific). Quantification was performed by determining the number of immunoreactive cells per lesion area for Mac3 and CD3, or the number of immunoreactive cells/area of tunica media for SMA. Images were taken with a Zeiss AxioImager.Z1 microscope using AxioVision version 4.8.1.0 software. An AxioCam ICc3 camera was used and Objective lenses were Zeiss Plan-apochromat.

BM transplantation and high-fat diet

Six-week-old male *Neu1*^{hypo}*Apoe*$^{-/-}$ mice received septra antibiotic water and gelatin and were lethally irradiated with 1100 rad total body γ-irradiation. BM cells from *Apoe*$^{-/-}$ or *Neu1*^{hypo}*Apoe*$^{-/-}$ mice were prepared from femur and tibia bones in Iscove's modified Dulbecco's medium supplemented with penicillin, streptomycin, and amphotericin B (Life Technologies Inc., Burlington, ON). Irradiated mice received 1×10^6 BM cells by retro-orbital injection and were given septra antibiotic water and jello for 4 weeks following transplantation. The mice were then fed a high-fat diet (modified Stanford University diet with 21% butterfat, 0.15% cholesterol, and 1% safflower oil, from Dyets, Inc.) for 8 weeks, and were sacrificed for atherosclerosis and lipoprotein analyses. The transplantation efficiency was assessed by genotyping peripheral blood cells by PCR.

Peripheral blood immunophenotyping

Peripheral blood was collected from male *Apoe*$^{-/-}$ and *Neu1*^{hypo}*Apoe*$^{-/-}$ mice by terminal cardiac puncture with a heparinized needle. Erythrocytes were lysed using ACK lysis buffer, and the leukocytes were counted. Cells were then preincubated with 10 μg/ml of rat anti-mouse CD16/CD32 and immunostained for cell-surface markers using 1 μg of the following antibodies for 10^6 cells in FACS buffer (PBS, 0.2% BSA): hamster anti-mouse CD3ϵ-APC-Cy7 (clone 145-2C11), rat anti-mouse CD19-V450 (clone 1D3), and mouse anti-mouse NK1.1-PE-Cy7 (clone PK136). Separate reactions were used to assess hamster anti-mouse CD3ϵ-APC-Cy7 (clone 145-2C11), rat anti-mouse CD4-PE (clone GK1.5), rat anti-mouse Ly6C-v450 (clone AL-21), rat anti-mouse CD115-PE (clone AF598), and rat anti-mouse CD8a-Pacific Blue™ (clone 53-6.7). All antibodies were obtained from BD Biosciences. The samples were washed with FACS buffer, fixed with BD Cytofix™ Fixation Buffer (BD Biosciences, Mississauga, Canada), and washed again before being run on a LSR II flow cytometer (Beckman Coulter Canada, Mississauga, ON).

Selectin and hyaluronic acid-binding assay

Peripheral blood was isolated by cardiac puncture, and red blood cells were lysed using ACK lysis buffer (150 mM NH_4Cl, 10 mM $KHCO_3$, 100 mM Na_2EDTA). Cells were incubated in Hanks' balanced salt solution containing calcium and magnesium at 37 °C for 1 h with 4 μg of P-selectin-human IgG chimera, 4 μg of E-selectin-human IgG chimera (R&D Systems), or 200 μg of fluorescein-conjugated hyaluronic acid (Calbiochem, La Jolla, CA). To detect bound selectin chimera protein, cells were incubated on ice with anti-human IgG conjugated to Alexa Fluor 488 (Life Technologies). The cells were incubated on ice with hamster anti-mouse CD3ϵ-Pacific Blue (clone 145-2C11) and rat anti-mouse CD11b-APC (clone M1/70) to detect T cells and monocyte/granulocyte populations, respectively (BD Biosciences). Samples were fixed with BD Cytofix™ Fixation Buffer (BD Biosciences) and run on a LSR II flow cytometer (Beckman Coulter Canada).

Leukocyte recruitment

Neu1^{hypo} mice were left untreated or were tail vein injected with helper-dependent adenovirus containing a mouse sialidase gene or bacterial β-Gal cDNA (100 μl, 10^9 particles/mouse in sterile PBS). Generation of the adenovirus was described previously (20). After 4 weeks, C57BL/6 mice and *Neu1*^{hypo} mice (untreated and adenovirus treated) were injected intraperitoneally with TNFα (500 ng, BD Biosciences) and 4 h later, hepatic microcirculation was examined by intravital microscopy as described previously (51). Leukocytes were classified as adherent (stationary for 30 s) or rolling along the central vein endothelium. Data are expressed as the flux of rolling cells (number per minute per ×40 field of view) or the number of adherent cells per ×40 field of view. When the central vein did not exhibit flow for 30 s, cells were classified as having no flow.

Cell-surface protein expression assay

Human THP-1 monocytic cells were cultured in RPMI media supplemented with 10% FBS, penicillin/streptomycin, amphotericin B, and differentiated into macrophages using 200 nM phorbol 12-myristate 13-acetate for 3 days. Culture reagents were obtained from Life Technologies, Inc. The macrophages were incubated with LPS (1 μg/ml, Sigma) for 8 h in the presence or absence of DANA (200 and 500 μM, Toronto Research Chemicals). The cell-surface proteins were biotinylated and purified using the Pierce Cell Surface Protein Isolation Kit (Thermo Fisher Scientific Inc.), following the manufacturer's instructions. Proteins were separated by SDS-PAGE, and transferred to nitrocellulose before immunoblotting for mouse anti-human LAMP2 (H4B4, Developmental Studies Hybridoma Bank, University of Iowa), goat anti-GAPDH (R&D Systems), rabbit anti-human NEU1 (Rockland Immunochemicals Inc.), and rabbit anti-Na^+-K^+-ATPase and rabbit anti-CD44 (Cell Signaling Technology).

THP-1 hyaluronic acid-binding assay

THP-1 monocytes were differentiated during culture with 200 nM phorbol 12-myristate 13-acetate as described above.

Macrophages were left untreated or infected with 10^9 plaque-forming unit adenovirus expressing human NEU1 (Ad-sialidase) and cultured for 3 days before HA binding analysis. Cells were incubated with HA-fluorescein (Calbiochem) for 10 or 30 min before running samples on the flow cytometer.

Lectin precipitation of protein and analysis of CD44 sialylation

THP-derived macrophages were infected during culture with either AdFG140 (empty) or AdSial (human NEU1) adenoviruses, and used for further protocols 3 days post-infection. Macrophages were collected in lysis buffer (1% Nonidet P-40, 2 mM phenylmethylsulfonyl fluoride, 0.1% deoxycholate) containing protease inhibitor mixture (Roche Applied Science), and were incubated overnight with 10–20 μg of biotinylated lectins: *Maackia amurensis II* (MALII), *Sambucus nigra* (SNA), and *Peanut agglutinin* (PNA). All lectins were obtained from Vector Laboratories. Lectin-precipitated proteins were isolated from cell lysates using streptavidin beads (Amersham Biosciences, GE Healthcare Life Sciences). Following a 1-h incubation at 4 °C, beads were spun down at 13,000 rpm for 5 min and the pellet was resuspended three times in ice-cold PBS (Hyclone, GE Healthcare Life Sciences). Lectin-precipitated proteins were reduced in Laemmli sample buffer containing β-mercaptoethanol and boiled. Samples were separated by SDS-PAGE, transferred to nitrocellulose membrane (Pall Canada Ltd., Ville St. Laurent, QC), and incubated with anti-CD44 antibody (Santa Cruz Biotechnology, Santa Cruz, CA) overnight in 5% nonfat milk, TBST. Blots were incubated with HRP-labeled secondary antibody and signals were generated and visualized using ECL and Hyperfilm, respectively (Amersham Biosciences, GE Healthcare Life Sciences). Protein concentrations were determined using a Bio-Rad Protein Assay (Bio-Rad Laboratories Canada Ltd., Mississauga, ON).

Immunoblot analysis

Aorta and liver tissues were freshly isolated from 7- month-old *Apoe*$^{-/-}$ and *Neu1*^{hypo}*Apoe*$^{-/-}$ mice and homogenized in RIPA buffer containing protease inhibitors (Roche Applied Science). Protein concentration was determined using the DC™ Protein Assay (Bio-Rad Laboratories Canada Ltd.). Samples were separated by SDS-PAGE and transferred to nitrocellulose membrane using Tris glycine buffer. Primary rabbit anti-Neu1 sialidase (1:500, Rockland Immunochemicals, Inc.) or goat anti-mouse Gapdh (1:2000, R&D Systems) were incubated in 5% milk, TBST overnight at 4 °C with agitation. Secondary goat anti-rabbit IgG-HRP or donkey anti-goat IgG-HRP antibodies were incubated in 5% milk, TBST for 1 h. Signals were visualized with chemiluminescence (ECL, Amersham Biosciences, GE Healthcare) and exposed to Amersham Biosciences Hyperfilm ECL. Signal intensity was measured using ImageJ software.

Sialidase activity assay

Tissue was freshly isolated from mice perfused with PBS. Approximately 0.1 g of aorta and liver were minced on ice and briefly homogenized in 1.0 ml of water. For BMDMs, bone marrow isolated from *Apoe*$^{-/-}$ and *Neu1*^{hypo}*Apoe*$^{-/-}$ mice was cultured for 9 days in RPMI 1640 supplemented with 10% FBS, 10 mM HEPES, penicillin/streptomycin, amphotericin B, and 5 ng/ml of macrophage colony-stimulating factor (Gibco, Life Technologies Inc.). BMDMs were lysed in 100 μl of water, half was used for sialidase activity, whereas the remaining material was used to measure protein concentration. Tissue homogenate or lysed BMDMs were then incubated for 1 h at 37 °C in 0.9% BSA, 0.2 mM 2-(4-methylumbelliferyl)-α-D-*N*-acetylneuraminic acid (4-MU-NANA, Toronto Research Chemicals, Inc.) in acetate buffer at pH 4.2. The reaction was stopped by the addition of 0.1 M 2-amino-2-methyl-1-propanol buffer, pH 9.5. Enzyme activity was measured as the amount of fluorescence generated from the liberation of umbelliferone (4-MU) from the *N*-acetylneuraminic acid (NANA) substrate. Fluorescence was measured using a PerkinElmer fluorometer and normalized to protein concentration that was determined using the DC™ Protein Assay (Bio-Rad Laboratories Canada Ltd.).

Serum cytokine measurement

Male *Apoe*$^{-/-}$ and *Neu1*^{hypo}*Apoe*$^{-/-}$ mice were injected with 25 μg of anti-CD3ϵ antibody (clone 145-2C11, BD Pharmingen, Mississauga, ON) in sterile saline. Blood was harvested at 2, 4, and 8 h, in blood collection tubes, spun at 10,000 $\times$ *g* for 5 min and stored at −80 °C until analysis. For time 0 h, blood was collected from untreated animals and used to determine baseline levels. Serum IL-2, IL-4, IL-10, and IFNγ cytokine levels were analyzed according to the mouse Th1/Th2 Ready-SET-Go! ELISA Set (eBioscience, San Diego, CA).

Immunofluorescence

Heart tissues were fixed with 3.7% formaldehyde, flash frozen in Shandon™ Cryomatrix™, and sectioned using a Shandon cryostat (Thermo Fisher Scientific). Aortic root sections were thawed, blocked with 10% goat serum PBS, and incubated overnight at 4 °C with primary antibody in 1% goat serum PBS including rabbit anti-MCP-1 (1:100, number ab7202, Abcam Inc., Toronto, ON), or rat anti-VCAM-1 (cell culture supernatant from a rat B-lymphocyte hybridoma cell line engineered to produce antibody against mouse VCAM-1, CRL-1909, ATCC, Manassas, VA). Sections were washed and then incubated at room temperature for 1 h with secondary goat anti-rabbit IgG-Alexa 594 or goat anti-rat IgG-Alexa Fluor 594 (1:500, Molecular Probes, Burlington, ON). Sections were washed, incubated with 4′,6-diamidino-2-phenylindole nuclear stain, washed again, and mounted with coverslips using Prolong Anti-fade mounting medium (Molecular Probes, Burlington, ON). MCP-1 and VCAM-1 positive area and fluorescence intensity was measured using ImageJ software.

Statistical analysis

One-way analysis of variance was followed by Tukey's or Dunnett's multiple comparison tests, or Student's *t* test was used when appropriate. When heterogeneous variances were present, one-way analysis of variance or Student's *t* test with unequal-variance were used. Tests were conducted using Prism 5 (version 5.04, GraphPad, La Jolla, CA). Individual data were

presented when possible, with the mean ± S.D. Comparisons were considered significantly different if $p < 0.05$.

Author contributions—E. J. W. and B. T. data curation; E. J. W. and B. T. formal analysis; E. J. W., G. G., S. L., M. M. S., T. C., M. T. F., and A. E. F.-R. investigation; E. J. W. visualization; E. J. W., G. G., S. L., M. M. S., T. C., M. T. F., O. D., A. E. F.-R., R. C. A., and B. T. methodology; E. J. W., R. C. A., and B. T. writing-review and editing; T. C., B. T., and S. A. I. validation; R. C. A. resources; B. T. and S. A. I. supervision; S. A. I. conceptualization; S. A. I. funding acquisition; S. A. I. writing-original draft; S. A. I. project administration.

Acknowledgments—We thank Abraham Yang for performing lipoprotein analyses and atherosclerotic plaque size measurements and additional technical assistance. We acknowledge the technical assistance provided by Aline Fiebig, Sheila Brown, and Darren DeSa.

References

1. Weber, C., and Noels, H. (2011) Atherosclerosis: current pathogenesis and therapeutic options. *Nat. Med.* **17,** 1410–1422 CrossRef Medline
2. Liang, F., Seyrantepe, V., Landry, K., Ahmad, R., Ahmad, A., Stamatos, N. M., and Pshezhetsky, A. V. (2006) Monocyte differentiation up-regulates the expression of the lysosomal sialidase, Neu1, and triggers its targeting to the plasma membrane via major histocompatibility complex class II-positive compartments. *J. Biol. Chem.* **281,** 27526–27538 CrossRef Medline
3. Stamatos, N. M., Liang, F., Nan, X., Landry, K., Cross, A. S., Wang, L. X., and Pshezhetsky, A. V. (2005) Differential expression of endogenous sialidases of human monocytes during cellular differentiation into macrophages. *FEBS J.* **272,** 2545–2556 CrossRef Medline
4. Cross, A. S., Sakarya, S., Rifat, S., Held, T. K., Drysdale, B. E., Grange, P. A., Cassels, F. J., Wang, L. X., Stamatos, N., Farese, A., Casey, D., Powell, J., Bhattacharjee, A. K., Kleinberg, M., and Goldblum, S. E. (2003) Recruitment of murine neutrophils *in vivo* through endogenous sialidase activity. *J. Biol. Chem.* **278,** 4112–4120 CrossRef Medline
5. Sakarya, S., Rifat, S., Zhou, J., Bannerman, D. D., Stamatos, N. M., Cross, A. S., and Goldblum, S. E. (2004) Mobilization of neutrophil sialidase activity desialylates the pulmonary vascular endothelial surface and increases resting neutrophil adhesion to and migration across the endothelium. *Glycobiology* **14,** 481–494 CrossRef Medline
6. Pappu, B. P., and Shrikant, P. A. (2004) Alteration of cell surface sialylation regulates antigen-induced naive CD8+ T cell responses. *J. Immunol.* **173,** 275–284 CrossRef Medline
7. Achyuthan, K. E., and Achyuthan, A. M. (2001) Comparative enzymology, biochemistry and pathophysiology of human exo-α-sialidases (neuraminidases). *Comp. Biochem. Physiol. B Biochem. Mol. Biol.* **129,** 29–64 CrossRef Medline
8. Igdoura, S. A., Gafuik, C., Mertineit, C., Saberi, F., Pshezhetsky, A. V., Potier, M., Trasler, J. M., and Gravel, R. A. (1998) Cloning of the cDNA and gene encoding mouse lysosomal sialidase and correction of sialidase deficiency in human sialidosis and mouse SM/J fibroblasts. *Hum. Mol. Genet.* **7,** 115–121 CrossRef Medline
9. Pshezhetsky, A. V., Richard, C., Michaud, L., Igdoura, S., Wang, S., Elsliger, M. A., Qu, J., Leclerc, D., Gravel, R., Dallaire, L., and Potier, M. (1997) Cloning, expression and chromosomal mapping of human lysosomal sialidase and characterization of mutations in sialidosis. *Nat. Genet.* **15,** 316–320 CrossRef Medline
10. Monti, E., Preti, A., Rossi, E., Ballabio, A., and Borsani, G. (1999) Cloning and characterization of NEU2, a human gene homologous to rodent soluble sialidases. *Genomics* **57,** 137–143 CrossRef Medline
11. Miyagi, T., Wada, T., Iwamatsu, A., Hata, K., Yoshikawa, Y., Tokuyama, S., and Sawada, M. (1999) Molecular cloning and characterization of a plasma membrane-associated sialidase specific for gangliosides. *J. Biol. Chem.* **274,** 5004–5011 CrossRef Medline
12. Comelli, E. M., Amado, M., Lustig, S. R., and Paulson, J. C. (2003) Identification and expression of Neu4, a novel murine sialidase. *Gene* **321,** 155–161 CrossRef Medline
13. Champigny, M. J., Perry, R., Rudnicki, M., and Igdoura, S. A. (2005) Overexpression of MyoD-inducible lysosomal sialidase (neu1) inhibits myogenesis in C2C12 cells. *Exp. Cell Res.* **311,** 157–166 CrossRef Medline
14. Gadhoum, S. Z., and Sackstein, R. (2008) CD15 expression in human myeloid cell differentiation is regulated by sialidase activity. *Nat. Chem. Biol.* **4,** 751–757 CrossRef Medline
15. Gee, K., Kozlowski, M., and Kumar, A. (2003) Tumor necrosis factor-α induces functionally active hyaluronan-adhesive CD44 by activating sialidase through p38 mitogen-activated protein kinase in lipopolysaccharide-stimulated human monocytic cells. *J. Biol. Chem.* **278,** 37275–37287 CrossRef Medline
16. Malmendier, C. L., Delcroix, C., and Fontaine, M. (1980) Effect of sialic acid removal on human low density lipoprotein catabolism *in vivo*. *Atherosclerosis* **37,** 277–284 CrossRef Medline
17. Orekhov, A. N., Tertov, V. V., and Mukhin, D. N. (1991) Desialylated low density lipoprotein–naturally occurring modified lipoprotein with atherogenic potency. *Atherosclerosis* **86,** 153–161 CrossRef Medline
18. Ruelland, A., Gallou, G., Legras, B., Paillard, F., and Cloarec, L. (1993) LDL sialic acid content in patients with coronary artery disease. *Clin. Chim. Acta* **221,** 127–133 CrossRef Medline
19. Sprague, E. A., Moser, M., Edwards, E. H., and Schwartz, C. J. (1988) Stimulation of receptor-mediated low density lipoprotein endocytosis in neuraminidase-treated cultured bovine aortic endothelial cells. *J. Cell. Physiol.* **137,** 251–262 CrossRef Medline
20. Yang, A., Gyulay, G., Mitchell, M., White, E., Trigatti, B. L., and Igdoura, S. A. (2012) Hypomorphic sialidase expression decreases serum cholesterol by down-regulation of VLDL production in mice. *J. Lipid Res.* **53,** 2573–2585 CrossRef Medline
21. Potier, M., Lu Shun Yan, D., and Womack, J. E. (1979) Neuraminidase deficiency in the mouse. *FEBS Lett.* **108,** 345–348 CrossRef Medline
22. Carrillo, M. B., Milner, C. M., Ball, S. T., Snoek, M., and Campbell, R. D. (1997) Cloning and characterization of a sialidase from the murine histocompatibility-2 complex: low levels of mRNA and a single amino acid mutation are responsible for reduced sialidase activity in mice carrying the Neu1a allele. *Glycobiology* **7,** 975–986 CrossRef Medline
23. Champigny, M. J., Mitchell, M., Fox-Robichaud, A., Trigatti, B. L., and Igdoura, S. A. (2009) A point mutation in the neu1 promoter recruits an ectopic repressor, Nkx3.2 and results in a mouse model of sialidase deficiency. *Mol. Genet. Metab.* **97,** 43–52 CrossRef Medline
24. de Geest, N., Bonten, E., Mann, L., de Sousa-Hitzler, J., Hahn, C., and d'Azzo, A. (2002) Systemic and neurologic abnormalities distinguish the lysosomal disorders sialidosis and galactosialidosis in mice. *Hum. Mol. Genet.* **11,** 1455–1464 CrossRef Medline
25. Meindl, P., Bodo, G., Palese, P., Schulman, J., and Tuppy, H. (1974) Inhibition of neuraminidase activity by derivatives of 2-deoxy-2,3-dehydro-*N*-acetylneuraminic acid. *Virology* **58,** 457–463 CrossRef Medline
26. Katoh, S., Miyagi, T., Taniguchi, H., Matsubara, Y., Kadota, J., Tominaga, A., Kincade, P. W., Matsukura, S., and Kohno, S. (1999) Cutting edge: an inducible sialidase regulates the hyaluronic acid binding ability of CD44-bearing human monocytes. *J. Immunol.* **162,** 5058–5061 Medline
27. Amith, S. R., Jayanth, P., Franchuk, S., Siddiqui, S., Seyrantepe, V., Gee, K., Basta, S., Beyaert, R., Pshezhetsky, A. V., and Szewczuk, M. R. (2009) Dependence of pathogen molecule-induced Toll-like receptor activation and cell function on Neu1 sialidase. *Glycoconj. J.* **26,** 1197–1212 CrossRef Medline
28. Stamatos, N. M., Carubelli, I., van de Vlekkert, D., Bonten, E. J., Papini, N., Feng, C., Venerando, B., d'Azzo, A., Cross, A. S., Wang, L. X., and Gomatos, P. J. (2010) LPS-induced cytokine production in human dendritic cells is regulated by sialidase activity. *J. Leukoc. Biol.* **88,** 1227–1239 CrossRef Medline
29. Orekhov, A. N., Tertov, V. V., Sobenin, I. A., Smirnov, V. N., Via, D. P., Guevara, J., Jr., Gotto, A. M., Jr., and Morrisett, J. D. (1992) Sialic acid content of human low density lipoproteins affects their interaction with cell receptors and intracellular lipid accumulation. *J. Lipid Res.* **33,** 805–817 Medline

30. Millar, J. S. (2001) The sialylation of plasma lipoproteins. *Atherosclerosis* **154,** 1–13 CrossRef Medline
31. Filipovic, I., Schwarzmann, G., Mraz, W., Wiegandt, H., and Buddecke, E. (1979) Sialic-acid content of low-density lipoproteins controls their binding and uptake by cultured cells. *Eur. J. Biochem.* **93,** 51–55 CrossRef
32. Gayral, S., Garnotel, R., Castaing-Berthou, A., Blaise, S., Fougerat, A., Berge, E., Montheil, A., Malet, N., Wymann, M. P., Maurice, P., Debelle, L., Martiny, L., Martinez, L. O., Pshezhetsky, A. V., Duca, L., and Laffargue, M. (2014) Elastin-derived peptides potentiate atherosclerosis through the immune Neu1-PI3Kγ pathway. *Cardiovasc. Res.* **102,** 118–127 CrossRef Medline
33. Mochizuki, S., Brassart, B., and Hinek, A. (2002) Signaling pathways transduced through the elastin receptor facilitate proliferation of arterial smooth muscle cells. *J. Biol. Chem.* **277,** 44854–44863 CrossRef Medline
34. Soehnlein, O. (2012) Multiple roles for neutrophils in atherosclerosis. *Circ. Res.* **110,** 875–888 CrossRef Medline
35. Drechsler, M., Megens, R. T., van Zandvoort, M., Weber, C., and Soehnlein, O. (2010) Hyperlipidemia-triggered neutrophilia promotes early atherosclerosis. *Circulation* **122,** 1837–1845 CrossRef Medline
36. Sperandio, M., Gleissner, C. A., and Ley, K. (2009) Glycosylation in immune cell trafficking. *Immunol. Rev.* **230,** 97–113 CrossRef Medline
37. Katoh, S., Zheng, Z., Oritani, K., Shimozato, T., and Kincade, P. W. (1995) Glycosylation of CD44 negatively regulates its recognition of hyaluronan. *J. Exp. Med.* **182,** 419–429 CrossRef Medline
38. Linton, M. F., Atkinson, J. B., and Fazio, S. (1995) Prevention of atherosclerosis in apolipoprotein E-deficient mice by bone marrow transplantation. *Science* **267,** 1034–1037 CrossRef Medline
39. Lo, J. C., Wang, Y., Tumanov, A. V., Bamji, M., Yao, Z., Reardon, C. A., Getz, G. S., and Fu, Y. X. (2007) Lymphotoxin β receptor-dependent control of lipid homeostasis. *Science* **316,** 285–288 CrossRef Medline
40. Hong, C., and Tontonoz, P. (2008) Coordination of inflammation and metabolism by PPAR and LXR nuclear receptors. *Curr. Opin. Genet. Dev.* **18,** 461–467 CrossRef Medline
41. Yvan-Charvet, L., Pagler, T., Gautier, E. L., Avagyan, S., Siry, R. L., Han, S., Welch, C. L., Wang, N., Randolph, G. J., Snoeck, H. W., and Tall, A. R. (2010) ATP-binding cassette transporters and HDL suppress hematopoietic stem cell proliferation. *Science* **328,** 1689–1693 CrossRef Medline
42. Bonnet, P., and Bryce, R. A. (2004) Molecular dynamics and free energy analysis of neuraminidase-ligand interactions. *Protein Sci.* **13,** 946–957 CrossRefMedline
43. Cross, A. S., Hyun, S. W., Miranda-Ribera, A., Feng, C., Liu, A., Nguyen, C., Zhang, L., Luzina, I. G., Atamas, S. P., Twaddell, W. S., Guang, W., Lillehoj, E. P., Puché, A. C., Huang, W., Wang, L. X., Passaniti, A., and Goldblum, S. E. (2012) NEU1 and NEU3 sialidase activity expressed in human lung microvascular endothelia: NEU1 restrains endothelial cell migration, whereas NEU3 does not. *J. Biol. Chem.* **287,** 15966–15980 CrossRef Medline
44. Nohle, U., Beau, J. M., and Schauer, R. (1982) Uptake, metabolism and excretion of orally and intravenously administered, double-labeled *N*-glycoloylneuraminic acid and single-labeled 2-deoxy-2,3-dehydro-*N*-acetylneuraminic acid in mouse and rat. *Eur. J. Biochem.* **126,** 543–548 CrossRef Medline
45. Folch, J., Lees, M., and Sloane Stanley, G. H. (1957) A simple method for the isolation and purification of total lipides from animal tissues. *J. Biol. Chem.* **226,** 497–509 Medline
46. Millar, J. S., Cromley, D. A., McCoy, M. G., Rader, D. J., and Billheimer, J. T. (2005) Determining hepatic triglyceride production in mice: comparison of poloxamer 407 with Triton WR-1339. *J. Lipid Res.* **46,** 2023–2028 CrossRef Medline
47. Kuipers, F., Jong, M. C., Lin, Y., Eck, M., Havinga, R., Bloks, V., Verkade, H. J., Hofker, M. H., Moshage, H., Berkel, T. J., Vonk, R. J., and Havekes, L. M. (1997) Impaired secretion of very low density lipoprotein-triglycerides by apolipoprotein E- deficient mouse hepatocytes. *J. Clin. Investig.* **100,** 2915–2922 CrossRef Medline
48. Li, X., Catalina, F., Grundy, S. M., and Patel, S. (1996) Method to measure apolipoprotein B-48 and B-100 secretion rates in an individual mouse: evidence for a very rapid turnover of VLDL and preferential removal of B-48- relative to B-100-containing lipoproteins. *J. Lipid Res.* **37,** 210–220 Medline
49. Covey, S. D., Krieger, M., Wang, W., Penman, M., and Trigatti, B. L. (2003) Scavenger receptor class B type I-mediated protection against atherosclerosis in LDL receptor-negative mice involves its expression in bone marrow-derived cells. *Arterioscler. Thromb. Vasc. Biol.* **23,** 1589–1594 CrossRef Medline
50. Zhou, J., Lhotak, S., Hilditch, B. A., and Austin, R. C. (2005) Activation of the unfolded protein response occurs at all stages of atherosclerotic lesion development in apolipoprotein E-deficient mice. *Circulation* **111,** 1814–1821 CrossRef Medline
51. Fox-Robichaud, A., and Kubes, P. (2000) Molecular mechanisms of tumor necrosis factor α-stimulated leukocyte recruitment into the murine hepatic circulation. *Hepatology* **31,** 1123–1127 CrossRef Medline